An inhibitor of the proteasomal deubiquitinating enzyme USP14 induces tau elimination in cultured neurons

Received for publication, August 31, 2017 Published, Papers in Press, September 26, 2017, DOI 10.1074/jbc.M117.815126

Monica Boselli[‡1], Byung-Hoon Lee[‡§1], Jessica Robert[‡], Miguel A. Prado[‡], Sang-Won Min[¶], Chialin Cheng[‖], M. Catarina Silva[‖], Changhyun Seong[‡], Suzanne Elsasser[‡], Ketki M. Hatle[‡], Timothy C. Gahman[‡‡], Steven P. Gygi[‡], Stephen J. Haggarty[‖], Li Gan[¶], Randall W. King[‡2], and Daniel Finley[‡3]**

*From the [‡]Department of Cell Biology, Harvard Medical School, Boston, Massachusetts 02115, the [§]Department of New Biology, Daegu Gyeongbuk Institute of Science and Technology, 42988 Daegu, Korea, the [¶]Department of Neurology, Gladstone Institute of Neurological Diseases, University of California, San Francisco, California 94158, [‖]Chemical Neurobiology Laboratory, Center for Genomic Medicine, Department of Neurology, Massachusetts General Hospital, Harvard Medical School, Boston, Massachusetts 02114, **Regeneron Pharmaceuticals, Tarrytown, New York 10591, and [‡‡]Small Molecule Discovery Program, Ludwig Institute for Cancer Research, La Jolla, California 92093*

Edited by George N. DeMartino

The ubiquitin-proteasome system (UPS) is responsible for most selective protein degradation in eukaryotes and regulates numerous cellular processes, including cell cycle control and protein quality control. A component of this system, the deubiquitinating enzyme USP14, associates with the proteasome where it can rescue substrates from degradation by removal of the ubiquitin tag. We previously found that a small-molecule inhibitor of USP14, known as IU1, can increase the rate of degradation of a subset of proteasome substrates. We report here the synthesis and characterization of 87 variants of IU1, which resulted in the identification of a 10-fold more potent USP14 inhibitor that retains specificity for USP14. The capacity of this compound, IU1-47, to enhance protein degradation in cells was tested using as a reporter the microtubule-associated protein tau, which has been implicated in many neurodegenerative diseases. Using primary neuronal cultures, IU1-47 was found to accelerate the rate of degradation of wild-type tau, the pathological tau mutants P301L and P301S, and the A152T tau variant. We also report that a specific residue in tau, lysine 174, is critical for the IU1-47–mediated tau degradation by the proteasome. Finally, we show that IU1-47 stimulates autophagic flux in primary neurons. In summary, these findings provide a powerful research tool for investigating the complex biology of USP14.

The ubiquitin-proteasome system (UPS)[4] is the major cellular pathway responsible for selective protein degradation within the eukaryotic cell (1–4). Proteins destined for elimination typically carry covalent ubiquitin modifications, which can serve as recognition signals for the proteasome as well as for selective autophagy. The formation of a substrate-bound ubiquitin chain requires the activity of three classes of enzymes: ubiquitin-activating enzyme (E1), which activates the carboxyl terminus of ubiquitin; a ubiquitin-conjugating enzyme (E2), which receives ubiquitin from E1, forming a thioester adduct; and a ubiquitin-protein ligase (E3), which binds substrates and guides the donation of ubiquitin from the E2. The serial addition of ubiquitin to a substrate through this pathway, often forming ubiquitin chains, generates substrates of progressively higher affinity for the proteasome and thus more rapid rates of degradation. The proteasome recognizes substrates via specific ubiquitin receptors within its 19-subunit regulatory particle. Subsequently, in an ATP-dependent process, the proteasome translocates the substrate into the 28-subunit core particle to be degraded (2, 5, 6).

Integral subunits of the proteasome are complemented by a variety of proteins that associate with it in a salt-sensitive manner and that are not stoichiometric within the complex (7). These proteasome-associated proteins regulate protein degradation in diverse ways; they include both inhibitors and activators of the proteasome as well as factors that alter its specificity. Among these factors, a deubiquitinating enzyme (DUB) known

This work was supported by a grant from the Tau Consortium (to D. F. and S. J. H.); by National Institutes of Health Grants R01 GM095526 and GM043601 (to D. F.), R01 GM66492 (to R. W. K.), and R01 AG054214 (to L. G.); and by the Basic Science Research Program through the National Research Foundation of Korea funded by Ministry of Science and Information Communication and Technology (ICT) Grant 2017R1A2B4006671, a Daegu Gyeongbuk Institute of Science and Technology start-up fund, and High Risk High Return, Ministry of Science, ICT, and Future Planning Grants 2017010074 and 2017010133 (to B.-H. L.). Patents 8933087 and 9201073 are held on IU1, IU1-47, and USP14 inhibition. A patent application on this work has been filed by Harvard University on behalf of the authors. The content is solely the responsibility of the authors and does not necessarily represent the official views of the National Institutes of Health.

This article contains supplemental Figs. 1–7 and Tables 1 and 2.

[1] Both authors contributed equally to this work.

[2] To whom correspondence may be addressed: Dept. of Cell Biology, Harvard Medical School, 240 Longwood Ave., Boston, MA 02115. Tel.: 617-432-3692; Fax: 617-432-1144; E-mail: randy_king@hms.harvard.edu.

[3] To whom correspondence may be addressed: Dept. of Cell Biology, Harvard Medical School, 240 Longwood Ave., Boston, MA 02115. Tel.: 617-432-3492; Fax: 617-432-1144; E-mail: daniel_finley@hms.harvard.edu.

[4] The abbreviations used are: UPS, ubiquitin-proteasome system; DUB, deubiquitinating enzyme; MEF, murine embryonic fibroblast; MAPT, microtubule-associated protein tau; htau, human tau; Ub-AMC, ubiquitin 7-amido-4-methylcoumarin; DIV, day(s) *in vitro*; AD, Alzheimer's disease; AQUA, absolute quantification; AAV, adeno-associated virus; FTD, frontotemporal dementia; FTDP-17, frontotemporal dementia and parkinsonism linked to chromosome 17; APP, amyloid precursor protein; PSEN1, presenilin; FAD, familial Alzheimer's disease; iPSC, induced pluripotent stem cell; ANOVA, analysis of variance; NPC, neural progenitor cell line; LC3, microtubule-associated protein 1B light chain 3.

in mammals as USP14 and in yeast as Ubp6, shows particularly strong regulation of the proteasome. USP14 and Ubp6 are profoundly activated upon association with the proteasome (7–9). Substrate deubiquitination by USP14 and Ubp6 can be very fast, and accordingly the suppression of proteasome activity by deubiquitination appears to result from the removal of ubiquitin from the substrate before the proteasome commits to degrading the substrate component of the ubiquitin-protein conjugate (8); lacking the ubiquitin tether, the substrate may be released prematurely. Although most USP14 substrates are likely to be docked on the proteasome, there is evidence that USP14 suppresses autophagy as well through an unknown mechanism (10).

The phenotype of mouse *Usp14* mutants indicates that it is particularly important in neurons (11–13), although phenotypic severity is highly strain-dependent (14). Consistent with a noncatalytic function of the enzyme, as described originally for the yeast ortholog (9, 15), the Usp14 loss-of-function phenotype in the mouse may not entirely reflect loss of deubiquitinating activity as indicated by studies involving transgenic overexpression of a catalytically inactive form of the enzyme (13, 16).

We previously identified specific small-molecule inhibitors of human USP14 by high-throughput screening. One such compound, known as IU1, abrogates the catalytic activity of USP14 while apparently not affecting its noncatalytic regulatory function (8). IU1 is cytoprotective under various conditions, including ischemia–reperfusion and endoplasmic reticulum stress (17, 18). Using murine embryonic fibroblast (MEF) and HEK293 cells, IU1 was shown to accelerate the degradation of some but not all substrates of the proteasome (8). Consistent with the selectivity of USP14's effect on protein degradation in cells, preferred *in vitro* substrates of USP14 are modified by multiple ubiquitin chains (8, 19). USP14 removes chains en bloc until a single chain remains but will not remove the last chain.

The availability of IU1 has led to the identification of a growing number of proteins identified as apparent targets of USP14's deubiquitinating activity. Proteins such as the androgen receptor, cyclic GMP-AMP synthase, vimentin, GFP^u, CD3δ, and most notably the prion protein Prp^C show accelerated degradation or reduced levels upon IU1 treatment, most simply accounted for by reduced deubiquitination at the proteasome (17, 20–24). Interestingly, IU1 specifically reduces the level of a phosphorylated form of tyrosine hydroxylase (25). Thus, USP14 inhibition enhances protein degradation *in vivo* and *in vitro* (8, 19), although, likely because of the sharply restricted substrate specificity of USP14 (19), its inhibition does not enhance the degradation of proteins generally. Consistent with this view, USP14 knockdown resulted in reduced levels of 87 proteins in H4 neuroglioma cells (10). In addition, MEFs that are null for USP14 showed accelerated bulk degradation of proteins (26). Assuming that these effects are direct, they might be due to abrogation of deubiquitination or of the noncatalytic effect of USP14.

Recent work has begun to explore the integration of USP14 into cellular signaling pathways. USP14 is phosphorylated by AKT at Ser-432 within the BL2 loop of USP14 (10), which occludes the USP14 active site in the inactive state of the enzyme (27). This phosphorylation event appears to increase the activity of proteasome-bound USP14 (10), although it may be insufficient to activate USP14 to disassemble ubiquitin-protein conjugates in the absence of the proteasome (19). In addition to AKT, the JNK and WNT signaling pathways have been linked to USP14 (13, 28).

Several key proteins involved in neurodegenerative diseases appear to be proteasome substrates (18, 29, 30). An example is the microtubule-associated protein tau (MAPT), which regulates microtubule assembly and stability (31, 32). Point mutations at several sites in the *MAPT* gene lead to familial frontotemporal dementia and parkinsonism linked to chromosome 17 (FTDP-17). Other diseases characterized by the accumulation of tau-containing protein aggregates include Alzheimer's disease, chronic traumatic encephalopathy, progressive supranuclear palsy, argyrophilic grain disease, corticobasal degeneration, and Pick's disease (33). Tau aggregates spread progressively through different brain regions, depending on the tauopathy (34). Tau is subject to extensive post-translational modification, including phosphorylation, acetylation, and ubiquitination. Tau toxicity appears closely linked to its acetylation and phosphorylation (35, 36).

Studies of tau-P301L transgenic mice harboring an inducible tau expression system showed that simple reduction in tau level is sufficient to restore performance in behavioral tests of memory and to prevent neuron loss (37). It is therefore of interest to investigate the use of small molecules that may be capable of selectively decreasing tau levels, several of which have been described (8, 35, 38). In the case of IU1, the molecular scaffold contains functional moieties that can be subjected to combinatorial chemical modifications to improve potency (Fig. 1*A*). We describe here 87 variants of IU1, among them IU1-47, a more potent inhibitor of USP14. Using tau as a reporter, we demonstrate that IU1-47 enhances protein degradation in neurons.

Results

IU1-47 is a potent and selective inhibitor of USP14

To develop a more potent USP14 inhibitor with improved selectivity, we prepared 87 analogs of IU1 (Fig. 1 and supplemental Tables 1 and 2). To evaluate selectivity, each derivative was tested in parallel for inhibition of USP14 and of IsoT/USP5, a closely related DUB, in both cases using the ubiquitin 7-amido-4-methylcoumarin (Ub-AMC) hydrolysis assay (8). Screening of IU1 variants was carried out in duplicate using a real-time fluorescence assay at a single concentration of compound. For those analogs that proved more potent than the parental compound, IC_{50} values were also determined (supplemental Table 1).

Of the initial set of analogs tested, most showed a severe reduction in USP14 inhibition, indicating that USP14 contacts across the landscape of IU1 must be preserved to retain activity (supplemental Table 1). A strong preference was observed for substitution at the 4-position of the fluorophenyl group (A-ring; Fig. 1*A*) with electron-withdrawing groups being favored, and an improvement in potency was correlated with increased lipophilicity (fluorine to chlorine). On the pyrrole core (B-ring; Fig. 1*A*), replacement of the methyl groups by hydrogen or ethyl moieties greatly reduced activity. Reduction

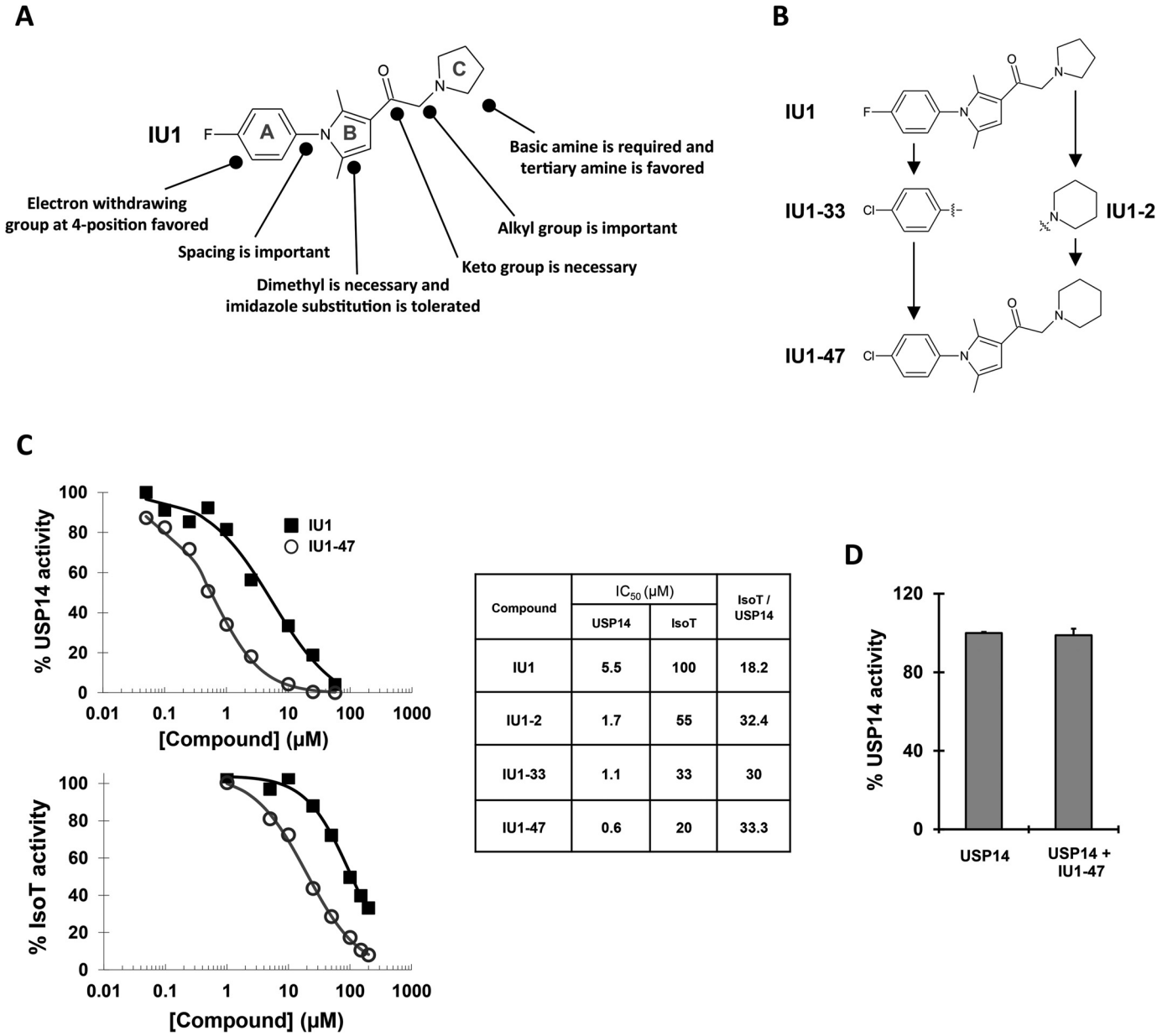

Compound	IC_{50} (μM)		IsoT / USP14
	USP14	IsoT	
IU1	5.5	100	18.2
IU1-2	1.7	55	32.4
IU1-33	1.1	33	30
IU1-47	0.6	20	33.3

Figure 1. IU1-47, a specific inhibitor of USP14 with improved potency. *A*, summary of structure–activity relationship analysis of IU1 derivatives (see also supplemental Tables 1 and 2). *B*, chemical structures of IU1-47 and related compounds. IU1-47 combines structural features of IU1-2 and IU1-33. *C*, dose-response curves for small-molecule inhibition of the Ub-AMC hydrolysis activity of proteasome-bound USP14 (*top left*) and IsoT/USP5 (*bottom left*), a closely related deubiquitinating enzyme (curves were fitted using nonlinear regression). Values correspond to the average of two duplicates. A representative example of $n > 3$ independent experiments is shown. A table of IC_{50} values of IU1 and its more potent derivatives is given at *right*. *D*, effect of IU1-47 (17 μM) on Ub-AMC hydrolysis activity of recombinant USP14 (2 μM) in the absence of proteasome. *Error bars* represent S.D.

of the ketone to either an alcohol or methylene completely eliminated USP14 inhibitory activity. Modification of the C-ring was tolerated with the tertiary amine favored over a secondary amine, although a secondary amine was not devoid of activity (Fig. 1*A* and see supplemental Table 1, IU1-4, IU1-6, IU1-8, IU1-14, IU1-15, and IU1-17). We found that piperidine (six-membered amine) was slightly more potent than pyrrolidine (five-membered amine). Replacement of the basic amine with an aniline abolished activity at the concentrations tested (supplemental Table 1, IU1-5 and IU1-16).

Among the first 37 analogs synthesized, we selected the most potent variations of the A- and C-rings and combined them to create IU1-47, 1-(1-(4-chlorophenyl)-2,5-dimethyl-1*H*-pyrrol-3-yl)-2-(piperidin-1-yl)ethanone (Fig. 1*B* and supplemental Table 1). IU1-47 has an IC_{50} value of 0.6 μM for proteasome-associated USP14 (Fig. 1*C*). This represents an ~10-fold increase in affinity for USP14 over IU1 accompanied by a modest increase in selectivity over IsoT/USP5 to ~33-fold (Fig. 1*C*). IU1-47 is more lipophilic than IU1 as reflected in its higher calculated log *P* value (5.9 as opposed to 4.7 in the case of IU1). The backbone of IU1-47 was further varied, although an analysis of 49 additional compounds yielded none that were appreciably improved in their properties (supplemental Table 2). Analytical studies, including ^{1}H NMR spectroscopic data of IU1-47 (supplemental Fig. 1), as well as liquid chromatography-mass spectrometry (LC-MS) analysis of IU1-47 and of its sta-

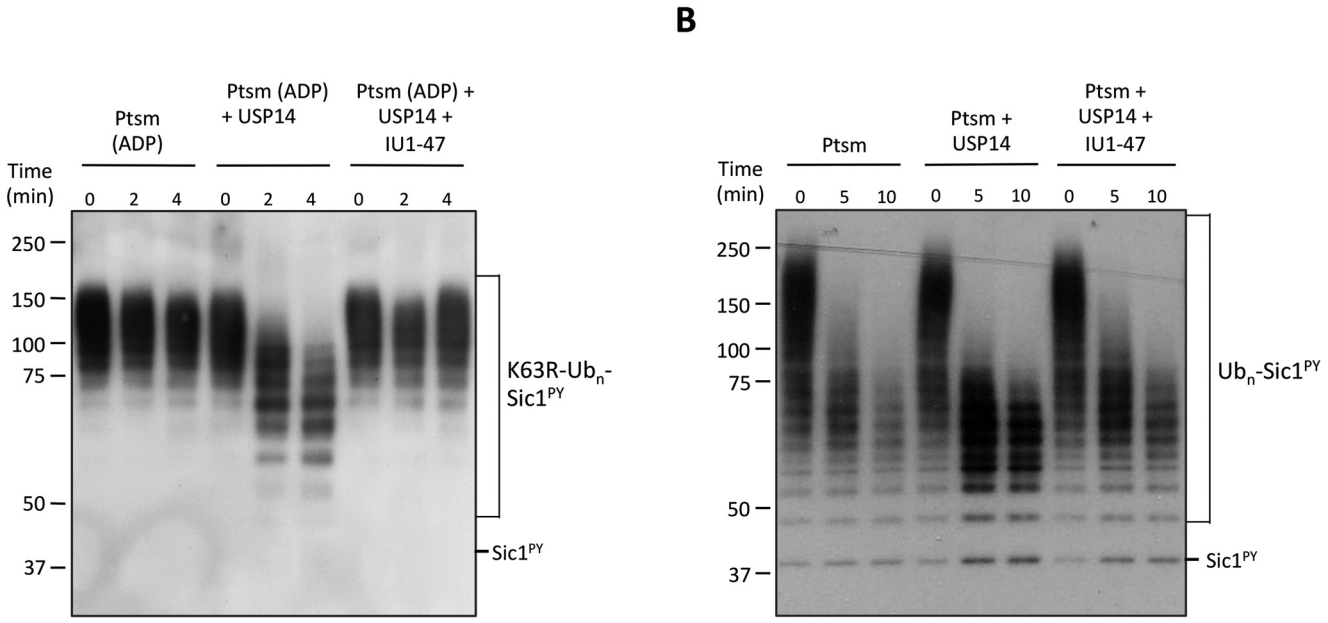

Figure 2. IU1-47 antagonizes USP14 deubiquitinating activity and stimulates substrate degradation *in vitro*. *A*, USP14-mediated deconjugation of polyubiquitinated T7-Sic1^{PY} by human proteasome (*Ptsm*) (4 nM) purified in the presence of ADP (*Ptsm (ADP)*) and with the addition of recombinant wild-type USP14 (80 nM). In these assays, ADP was further supplemented to 5 mM to suppress substrate degradation. Samples to which IU1-47 (17 μM) was added are indicated; control samples received the vehicle DMSO. Ub$_n$-Sic1^{PY} conjugates in this experiment were prepared using K63R ubiquitin. *B*, degradation of polyubiquitinated T7-Sic1^{PY} by USP14-free human proteasome (4 nM) and with the addition of recombinant wild-type USP14 (80 nM) in the presence or absence of IU1-47 (25 μM). This experiment was carried out in the presence of ATP (5 mM). Ub$_n$-Sic1^{PY} adducts were substantially rescued from degradation by the proteasome when USP14 was added. This effect is counteracted by IU1-47. A representative example of two independent experiments is shown.

bility in the presence of USP14 (supplemental Figs. 2 and 3, respectively) were also performed to confirm the purity and stability of the compound.

IU1-47 was essentially inactive on free USP14 (USP14 that is not bound to the proteasome) (Fig. 1*D*), consistent with our previous findings on the parental compound (8). The Ub-AMC hydrolytic activity of USP14 is enhanced 800-fold or more in the presence of proteasomes, indicating that proteasome-associated USP14 is in an activated state (8). Nonetheless, the Ub-AMC assay is sufficiently sensitive to monitor the activity of free USP14. In summary, failure to inhibit free USP14 is a shared feature of IU1 series compounds, evident over a range of potencies. Most likely these compounds probe a specific conformation of USP14 that is assumed upon proteasome binding.

IU1-47 enhances in vitro degradation of known proteasome substrates

We next tested the effect of IU1-47 on a proteasome substrate, the cyclin-dependent kinase inhibitor Sic1 (Fig. 2*A*). The Sic1 assay allows one to monitor *in vitro* the coupled USP14 activities of deubiquitination and modulation of substrate degradation rate. It has been shown that USP14 can inhibit the degradation of ubiquitinated Sic1^{PY} (8), an engineered form of Sic1 in which the PY element signals ubiquitination (39). We therefore tested whether IU1-47 could alleviate or reverse this effect. Initially, we assayed USP14-dependent deubiquitination under conditions that prevent substrate degradation; namely the proteasome was purified and assayed in the presence of ADP. Under these conditions, the deubiquitination of Sic1^{PY} is very rapid, almost reaching an apparent end point within 2 min (Fig. 2*A*). IU1-47 blocked this reaction, indicating that it inhibits USP14 activity against not only Ub-AMC but also against true ubiquitin-protein conjugates. In a similar experiment, we assayed the effect of IU1-47 on Sic1^{PY} in the presence of ATP where deubiquitination and substrate degradation proceed in parallel, thus competing to determine the fate of the substrate. As expected, USP14 strongly inhibited Sic1^{PY} degradation, and IU1-47 antagonized this effect (Fig. 2*B*). Comparable results were obtained using ubiquitinated cyclin B (19) as a substrate (data not shown).

IU1-47 decreases endogenous wild-type and human wild-type tau levels in cultured cells

IU1 is cell-permeable and stable in cultured cells (8). To determine whether the degradation of a proteolytic substrate could be stimulated in cells by inhibiting USP14 with IU1-47, we focused on tau (microtubule-associated protein tau), a protein implicated in neurodegenerative diseases (40–42). First, we transfected a plasmid that expresses wild-type, untagged human tau into both wild-type MEFs and MEFs lacking USP14. IU1-47 treatment increased tau degradation in wild-type MEFs, indicating that IU1-47 retains the capacity of IU1 to stimulate the degradation of specific proteasome substrates, consistent with our previous finding that IU1 affects tau degradation in MEFs (8). IU1-47 had no effect in this assay in *Usp14*-null MEFs, confirming that USP14 inhibition underlies stimulated tau degradation in this cell type (supplemental Fig. 4). Additionally, cell viability measured by 3-(4,5-dimethylthiazol-2yl)-2,5-diphenyltetrazolium bromide (MTT) assay showed that IU1-47 is well tolerated in MEFs (supplemental Fig. 5). The promotion of tau degradation by IU1-47 was independently observed using an adenoviral vector expressing wild-type human tau in MEFs (data not shown).

The toxic effect of mutant or misfolded tau is exerted in neurons (40, 42). The question of whether IU1-47 can be used to control tau levels in a physiologically relevant setting was assessed using primary neurons derived from either mouse or rat. Cortical primary neuronal cultures were infected with a lentiviral vector expressing wild-type human tau. At days *in vitro* (DIV) 9–12, cells were treated with IU1-47 and/or MG-132 for 48 h. Total tau levels were assessed by immunoblotting. IU1-47-treated cells showed a significantly lower level of tau, and the effect was reversed in the presence of the proteasome inhibitor MG-132, suggesting that IU1-47 stimulates tau degradation principally via the ubiquitin-proteasome system (Fig. 3*A*).

Hippocampal primary neurons were treated with IU1-47 for 48 h, and total tau, phosphotau, and non-phosphotau levels were assessed by quantitative immunoblotting (Fig. 3*B*). Phosphotau species were monitored because mutant forms of tau are known to be preferentially phosphorylated, and the pattern of tau phosphorylation correlates with the loss of neuronal integrity (43). We therefore assessed whether IU1-47 could promote the elimination of phosphotau species such as those detectable using the PHF1 and AT8 antibodies, which correlate with the later stages of disease progression in AD (43). As a result of IU1-47 treatment, all tau forms in primary neurons were significantly reduced, including the phosphorylated forms (Fig. 3*B*), presumably due to accelerated degradation of the phosphorylated species. Although all phosphorylated forms tested were reduced upon treatment, the IU1-47 effect was stronger for specific variants such as the Ser-202-phosphorylated species in comparison with those modified at Ser-396 and Ser-404. Similar results were obtained using cortical neurons, and IU1-47 proved significantly more potent than IU1 in these tau clearance assays (data not shown).

To confirm by an independent method that the tau level was indeed decreased upon IU1-47 treatment, we used absolute quantification (AQUA) for quantitative determination of total tau in cell lysates by LC-MS. For this approach, proteins present in extract were digested with Lys-C, and the abundance of a specific peptide from tau was compared with that of a synthetic heavy atom-labeled internal standard peptide of identical sequence. The analysis confirmed that the total tau level was indeed decreased upon IU1-47 treatment (Fig. 3*C*). As expected, the tau mRNA level was unaffected by IU1-47 treatment (Fig. 3*D*), and neuronal toxicity measured at the end of the 48-h treatment showed that murine primary neurons can tolerate IU1-47 treatment at the assayed concentrations (Fig. 3*E*).

Treatment with IU1-C (8), a structural analog of IU1-47 that fails to inhibit Ub-AMC hydrolysis, did not induce tau degradation (Fig. 3*F*). IU1, the progenitor of IU1-47, was much less effective than IU1-47 in this and other cell-based assays (data not shown).

IU1-47 stimulates degradation of human wild-type and pathological tau forms in murine primary neurons and in human induced pluripotent stem cell (iPSC)-derived neurons

Having studied the effects of IU1-47 on the turnover of endogenous wild-type tau, we examined the compound's effects on mutant forms of tau that cause neuronal toxicity. We tested IU1-47 treatment in primary neuronal cultures expressing human tau via an adeno-associated virus (AAV) system that codes for a pathogenic mutation, P301S, which has been shown to be causative for autosomal dominant FTDP-17 (44, 45). IU1-47 treatment decreased tau levels in these cultures as well (Fig. 4*A*). We then tested IU1-47 treatment using an AAV vector that expresses the A152T human tau variant (Fig. 4*B*), which has been proposed as a risk factor for both FTD and AD (46). A reduction in tau level comparable with what is shown in Fig. 4*A* was also observed for this tau variant (Fig. 4*B*).

We proceeded to use transgenic mice carrying the human tau mutation P301L (tau-P301L) and two additional mutations in the amyloid precursor protein (*APP*) gene and in the human presenilin (*PSEN1*) gene, both well studied in the context of AD (47, 48). These mice progressively develop both amyloid β and tau pathology, phenocopying both aspects of AD. We isolated primary cortical neuronal cultures from 3XFAD embryos and treated the cultures with IU1-47 as described above. Tau levels in primary neurons derived from these mice were significantly decreased upon treatment with IU1-47, including the phosphotau species Ser-202/Thr-205 (Fig. 4*C*). The level of USP14 itself did not change upon IU1-47 treatment of 3XFAD primary neurons (Fig. 4*C*) as is generally the case. Similar experiments were also performed using 5XFAD transgenic mice carrying six mutations in human genes associated with familial AD, including the human *APP* with the mutations K670N, M671L, I716V, and V717I and a human *PSEN1* transgene carrying the M146L and L286V mutations (49). By 6 months of age, these mice exhibit amyloid deposits, and they subsequently develop severe decreases in cognitive function. We isolated primary cortical neurons from 5XFAD mice and treated the resulting cultures with IU1-47 as described above. Under these conditions, both total tau and phosphotau were significantly decreased upon 48-h treatment with IU1-47 (Fig. 4*D*).

Finally, we tested whether tau reduction upon IU1-47 treatment was also observed in neurons derived from human iPSCs. Tau elimination upon IU1-47 treatment was also observed in human iPSC-derived neurons (Fig. 4*E*). Higher concentrations (~2–3×) and longer treatment times (96 *versus* 48 h) with IU1-47 were required for reduction of phosphotau levels in human iPSC-derived neurons as compared with rodent primary neurons. These higher exposure levels were still well tolerated (supplemental Fig. 6). Although these quantitative differences between rodent primary neurons and human iPSC-derived neurons in their responsiveness to IU1-47 may be attributable to species differences, they may alternatively reflect differences in the overall level of maturity of these cell populations. The former were treated with compound following approximately 1 week of *in vitro* culture (DIV4–6), whereas the latter were cultured for 6 weeks and under different conditions than primary neurons. In particular, human iPSC-derived neurons differ from their counterparts in the nature of the predominant tau species (whether 4R or 3R).

The effect of IU1-47 on proteasome-mediated degradation of tau is dependent on lysine 174

Recent work has shown the importance of lysine 174 in tau toxicity and turnover (50). We therefore tested whether IU1-47

can induce tau degradation in primary neuronal cultures expressing human tau mutant K174Q. Interestingly, IU1-47 induced the degradation of human wild-type tau but not its K174Q counterpart (Fig. 5*A*). We additionally performed an *in vivo* ubiquitination assay in HEK293 cells transiently expressing FLAG-tagged tau constructs (wild type, tau-K174Q, or tau-

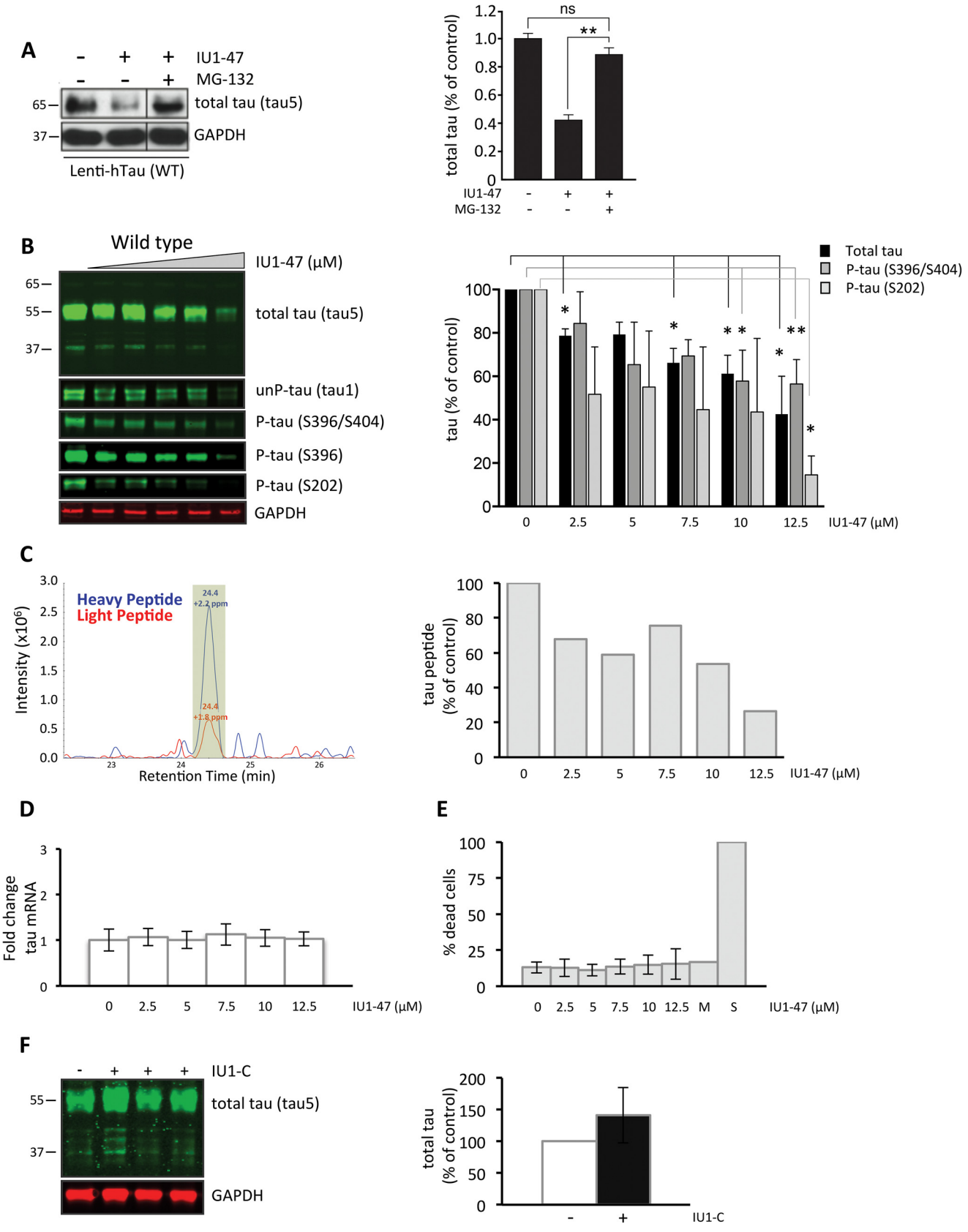

K274Q) and HA-tagged ubiquitin. Cells were treated with MG-132 to inhibit proteasomal degradation, and ubiquitinated tau was immunoprecipitated and detected with an antibody against the HA tag (Fig. 5*B*). The amount of polyubiquitinated tau-K174Q was significantly lower than that of its wild-type counterpart, confirming the importance of Lys0174 in proteasome-mediated degradation (Fig. 5*B*, *right panel*). A substitution of lysine 274 had no significant effect on the amount of polyubiquitinated tau in HEK293 cells, confirming the specificity of lysine 174 for tau-mediated degradation by the proteasome (Fig. 5*B*).

USP14 inhibition causes an increase in autophagic flux in primary neurons

Inhibition of USP14 has been shown to induce increased autophagic flux in neuroglioma cells (10). We therefore assessed whether IU1-47 also induced autophagy in primary neuronal cells. We observed a perturbation in autophagic flux as shown by elevation of the level of lipidated microtubule-associated protein 1B light chain 3 (LC3) in primary neuronal cultures treated with IU1-47 (Fig. 6*A*). We did not observe a marked difference of activated caspase-3 between vehicle-treated and IU1-47–treated samples, suggesting that IU1-47 did not induce apoptosis at the concentrations tested. In addition to proteasome-dependent degradation and autophagy, tau is subject to proteolytic cleavage by calpain in several cell types and tissues, including the brain (51–53). Calpain activation and subsequent tau cleavage result in a 17-kDa tau fragment (54). A recent study (55) tested the effects of the parental USP14 inhibitor IU1 in primary neurons and found that IU1 induces calpain activation and subsequent tau cleavage. This was found to be an off-target effect of IU1 and thus not relevant to USP14 inhibition. Using IU1-47, we did not observe the 17-kDa calpain-dependent cleavage fragment of tau detected with tau5 antibody (supplemental Fig. 7A) or with tau1 antibody (data not shown). In addition, we assessed whether calpain inhibition in primary neurons could abrogate the reduction in tau protein by IU1-47. Samples treated with both IU1-47 and calpeptin, a calpain inhibitor, were harvested and analyzed by immunoblotting. We found that samples treated with both IU1-47 and calpeptin showed a reduction in tau level similar to those treated with IU1-47 alone (Fig. 6*B*). Thus, IU1-47 does not appear to reduce tau levels through calpain activation at the concentrations and conditions used in this study. Our conditions differed from those of Kiprowska *et al.* (55) not only in the use of a different compound but also in the use of a different culture medium. For our experiments, all treatments were performed with Neurobasal medium because this neuronal cell-specific medium has previously been shown to improve neuronal cell viability compared with DMEM (56, 57). In accord with previous work, when we measured cell viability after subjecting cultures of primary neurons to cytotoxic stress using staurosporine, we found that viability was substantially higher in neurons subjected to stress in the presence of Neurobasal medium as compared with DMEM (supplemental Fig. 7B). The results suggest that medium formulation can influence neuronal response to chemical inhibitors. Taken together, our results show that, at the concentrations used, IU1-47 can enhance proteasome activity and selectively promote the degradation of specific substrates both *in vitro* and in cultured cells.

Discussion

Toxic misfolded proteins, often of mutant origin, are etiological agents in neurodegenerative diseases and in many other disorders. Given the prevalence of diseases of this type, collectively known as proteopathies, methods for reducing the levels of such damaging proteins are of potential interest. The elimination of misfolded proteins is a key function of the ubiquitin-proteasome pathway, and it is plausible that a significant fraction of proteopathic proteins are proteasome substrates although not necessarily preferred substrates. Thus, small molecules that enhance proteasome activity could have therapeutic value. Proteasome activity is held under negative control by deubiquitinating enzymes in that they remove the ubiquitin signal needed for effective targeting to the proteasome. Small-molecule inhibitors of USP14 and other deubiquitinating

Figure 3. IU1-47 treatment reduces the level of endogenous wild-type tau in murine primary neurons. *A*, rat primary cortical neurons were infected with lentiviral vector expressing human wild-type tau for 4 days. Cultures were then treated with either IU1-47 (25 μM) alone or in combination with MG-132 (10 μM) for 48 h. Lysates were prepared, and proteins were resolved by SDS-PAGE followed by immunoblot analysis at *left* to detect total tau (tau5 antibody). GAPDH was used as a loading control. The proteins' molecular masses are indicated. *Right*, quantification of IU1-47–mediated tau reduction ($n = 4$; treatment from two independent experiments). *Error bars* represent S.E. *Asterisks* denote $p < 0.01$ (one-way ANOVA, Tukey–Kramer post hoc analyses). *ns*, not significant. *B*, murine hippocampal primary neurons (DIV4) were incubated with graded doses of IU1-47 for 48 h. Lysates were prepared, resolved by SDS-PAGE, and immunoblotted with antibodies against endogenous total tau (tau5), unphosphorylated (*unP*) tau (tau1), and multiple forms of phosphorylated (*P*) tau (pSer-396/404, pSer-396, and pSer-202). GAPDH was used as a loading control. Proteins of interest were visualized with IRDye-conjugated secondary antibodies using an Odyssey imaging system (*left*). The proteins' molecular masses are indicated. The 37-kDa band is shown as it recognizes monomeric tau species detected with the tau5 antibody. Quantification of total tau (as detected by tau5 antibody) and of the phosphotau species pSer-396/404 (as detected by PHF1 antibody) and pSer-202 is shown for three independent experiments. *Error bars* represent S.D. *Asterisks* denote *p* values <0.05; *double asterisks* denote *p* values <0.01 of differences from appropriate DMSO controls (*right panel*). *C*, quantification by AQUA analysis of total tau level from whole-cell lysates of murine primary neurons treated with graded amounts of IU1-47. Elution profiles of heavy and light peptides resolved by LC-MS are shown with their retention time and mass errors (ppm). Peak heights are given in arbitrary units; intensity values have been divided by 10^6 for simplicity of presentation (*left*). Quantification was derived from the area under the curves, and values are given as a percentage of tau present as compared with lysate from DMSO-treated cells (*right*). *D*, quantitative PCR showing the level of tau transcript normalized to 18S rRNA and relative to DMSO-treated control after 48-h treatment with increasing concentrations of IU1-47 in mouse cortical primary neurons. Values correspond to the average of four replicates. *Error bars* represent S.D. *E*, viability of murine cortical primary neurons (DIV6) after 48-h treatment with IU1-47 was assayed using Toxilight bioassay (Lonza), which measures adenylate kinase activity released into the medium upon cell death. No treatment with medium alone and treatment with 1 μM staurosporine are indicated as *M* and *S*, respectively. Staurosporine, a nonselective kinase inhibitor that induces rapid programmed cell death in neurons, was used as a positive control for dead cells (84, 85). The graph shows neuronal viability upon IU1-47 treatment from three independent experiments. Values shown are averages, and *error bars* correspond to S.D. Measurements for medium alone and controls for dead cells were done in two of the three independent experiments. *F*, murine cortical primary neurons were treated with 12.5 μM IU1-C, a structural analog of IU1-47 that does not inhibit USP14, for 48 h. Lysates were prepared, resolved by SDS-PAGE, probed with antibodies against total tau (tau5) and GAPDH (loading control), and then visualized as above (*left*). Quantification of total tau indicates that there is no decrease in tau levels during the course of IU1-C treatment ($n = 3$; *right*). *Error bars* represent S.D.

enzymes have accordingly been found to stimulate the degradation of proteasome substrates (8, 10, 18, 20–22, 26, 58–62).

Almost 100 deubiquitinating enzymes are encoded in the human genome, providing myriad opportunities for modulating the output of the ubiquitin pathway (63–65), although it remains unclear what fraction of deubiquitinating enzymes play significant roles in negative regulation and how substrate-specific such effects may be. In some cases, potential applica-

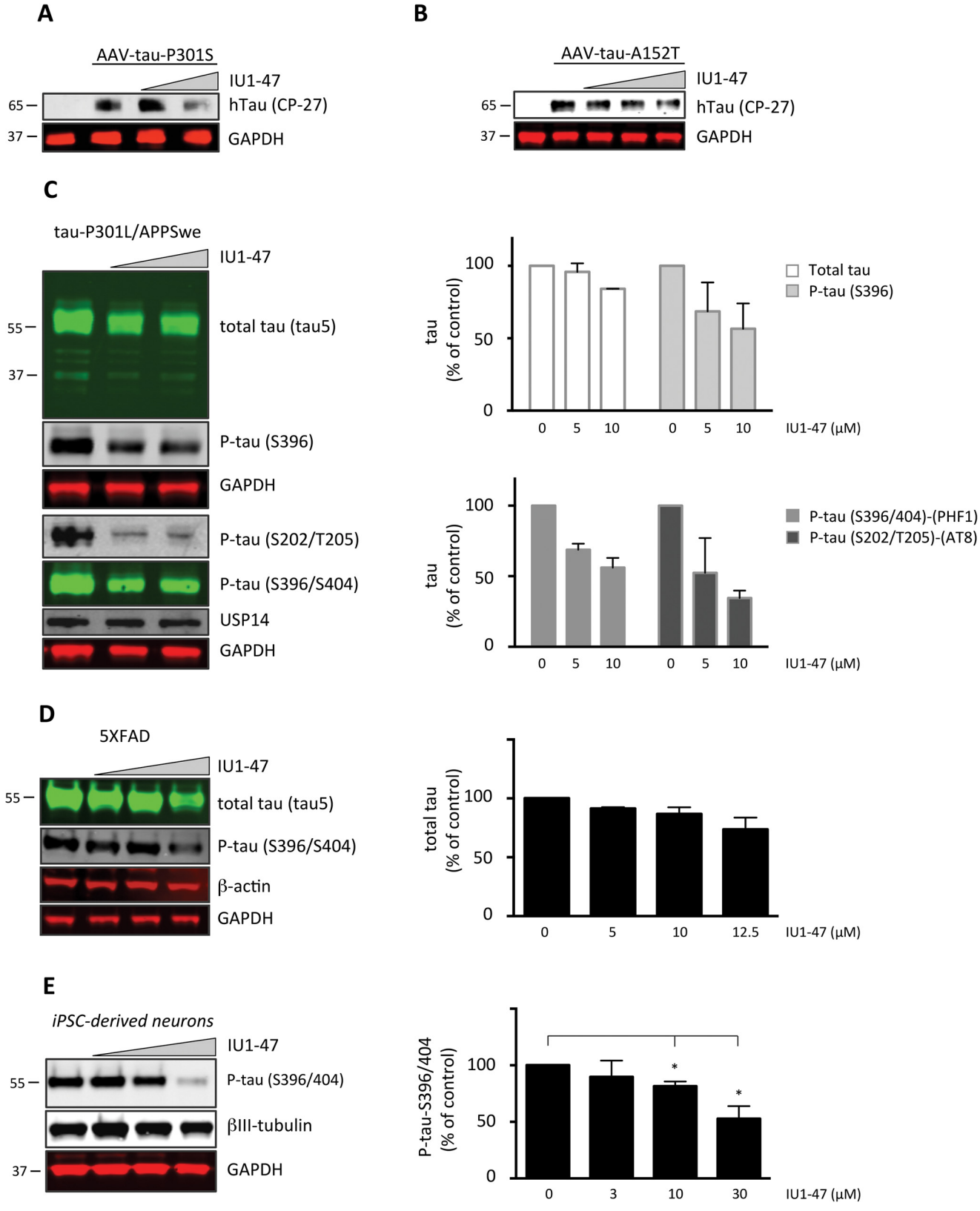

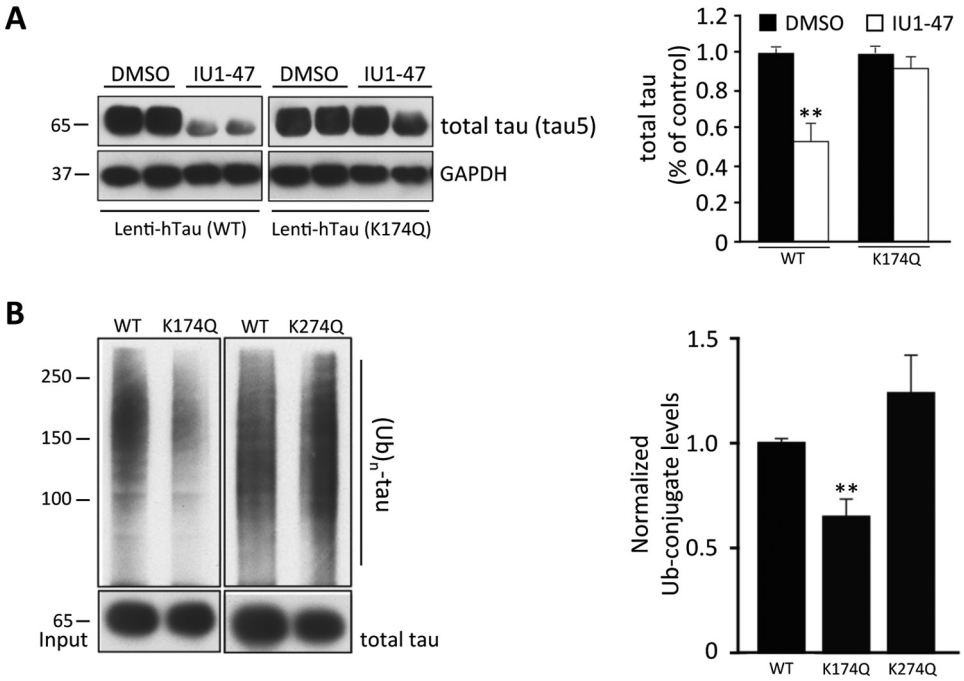

Figure 5. Lysine 174 of tau is required for IU1-47–mediated degradation. *A*, primary neurons were infected with AAV vectors that express either wild-type human tau or htau-K174Q. Four days after infection, the cultures were treated with either 25 μM IU1-47 or DMSO for 48 h. Cells were harvested, and lysates were prepared and resolved by SDS-PAGE. Total human tau was visualized by immunoblotting using the tau5 antibody. GAPDH was probed as a loading control. *Right*, quantification of IU1-47–mediated tau reduction is shown (htau wild type treated with DMSO ($n = 6$), htau wild type treated with IU1-47 ($n = 7$), htau-K174Q treated with DMSO ($n = 6$), and htau-K174Q treated with IU1-47 ($n = 7$) from four independent experiments). *Asterisks* denote $p < 0.01$ (Mann–Whitney nonparametric test). *Error bars* represent S.E. *B*, HEK293 cells were transfected with vectors expressing either FLAG-tagged human wild-type or mutant tau (K174Q or K274Q) and HA-ubiquitin. Cells were then treated with IU1-47 (10 μM) for 20 h and subsequently treated with MG-132 (20 μM) for 4 h. Cells were lysed with ubiquitination buffer, and supernatant proteins were immunoprecipitated with FLAG M2-agarose beads for 3 h. Reactions were resolved by SDS-PAGE and immunoblotted with anti-HA antibody. Tau5 antibody was used to detect total tau at the (*bottom left*). The *right panel* shows the quantification of polyubiquitinated tau normalized to total tau (wild-type tau ($n = 7$) and tau-K174Q ($n = 7$) from five independent experiments and tau-K274Q ($n = 5$) from two independent experiments). *Error bars* represent S.E. *Asterisks* denote $p < 0.01$ (one-way ANOVA, Tukey–Kramer post hoc analyses).

tions of DUB inhibitors in cancer chemotherapy are under investigation (66, 67).

One deubiquitinating enzyme that has been validated as a negative regulator of the proteasome is USP14. Its importance was highlighted first by studies of its yeast ortholog, Ubp6, which was discovered to be a potent endogenous inhibitor of the proteasome as well as a major proteasome component (7, 9, 15, 68). An unusual feature of this enzyme, as compared with other DUBs, is that its capacity to inhibit protein degradation requires a domain on Ubp6 that targets it to the proteasome (the Ubl domain) (7). Thus, Ubp6 is thought to remove ubiquitin from substrates that have already docked at the proteasome. The identification of a specific inhibitor of USP14, IU1, allowed for this paradigm to be extended to mammalian cells (8). IU1 has also been used to identify new functions of USP14's deubiquitinating activity (13, 28, 62, 69, 70), which in most cases remain to be elucidated in detail.

Figure 4. IU1-47 treatment reduces the level of pathological tau in primary neurons. *A*, rat cortical primary neurons were infected with AAV-tau-P301S, which expresses the human tau mutant P301S. After 5 days, IU1-47 was added at the indicated concentrations. Following an additional 2 days of culture, lysates were prepared, and proteins were resolved as described above. Human tau was visualized by immunoblotting using an antibody specific for human tau (CP-27), and GAPDH was probed as a loading control. The proteins' molecular masses are indicated. *B*, rat cortical primary neurons were infected with AAV-tau-A152T, which expresses human tau variant A152T, for 5 days prior to IU1-47 treatment for 48 h at the indicated concentrations. Lysates were prepared and resolved as described above. Human tau was visualized by immunoblotting using an antibody specific for human tau (CP-27), and GAPDH was probed as a loading control. *C*, murine cortical primary neurons (DIV5) isolated from APPSwe/P301L transgenic animals were incubated with the indicated doses of IU1-47 for 48 h, then harvested, and processed as above. Immunoblots developed with IRDye-conjugated secondary antibodies show the level of total tau and of several specific phospho (*P*)-tau species upon IU1-47 treatment. Phosphoepitopes are indicated in *parentheses*. The *top* three blots are from one gel; the *bottom* four blots are from another gel (*left*). The USP14 blot shows that no change in USP14 protein level was observed upon IU1-47 treatment. Values in the graphs represent an average of two biological replicates representing cortical neurons from littermates. *Error bars* represent S.E. (*right*). Monoclonal antibodies are listed below the matching epitope in the bar graph. *D*, murine cortical primary neurons (DIV6) isolated from 5XFAD mice were incubated with the indicated concentrations of IU1-47 for 48 h. Cells were harvested, and lysates were prepared and resolved as described above. A representative immunoblot shows the levels of total tau (as detected by tau5 antibody) in cortical neurons derived from one of two independently processed embryos upon treatment with IU1-47 (*left*). Secondary antibodies were IRDye-conjugated. The decrease in phosphorylated tau pSer-396/404 was also visualized with IRDye-conjugated secondary antibodies upon IU1-47 treatment. Quantification of total tau from independent samples is shown (*right*). *E*, NPC terminally differentiated into neurons for 6 weeks was treated with increasing concentrations of IU1-47. Lysates were prepared, resolved by SDS-PAGE, and immunoblotted with antibodies against phosphorylated tau (pSer-396/404). GAPDH was used as a loading control. βIII-tubulin levels were also assayed as a marker for differentiation and to assess cytoskeletal integrity. Proteins of interest were visualized with IRDye-conjugated secondary antibodies using an Odyssey imaging system. Similar results were obtained using an antibody against tau pSer-202 (not shown). Quantification of phosphotau (pSer-396/404) as detected by PHF1 (*right*) is shown for three independent experiments for the indicated time points or for two independent experiments. *Error bars* represent S.D. for $n = 3$ (DMSO and 10 and 30 μM IU1-47) and S.E. for $n = 2$ (3 μM IU1-47). *Asterisks* denote *p* values <0.05.

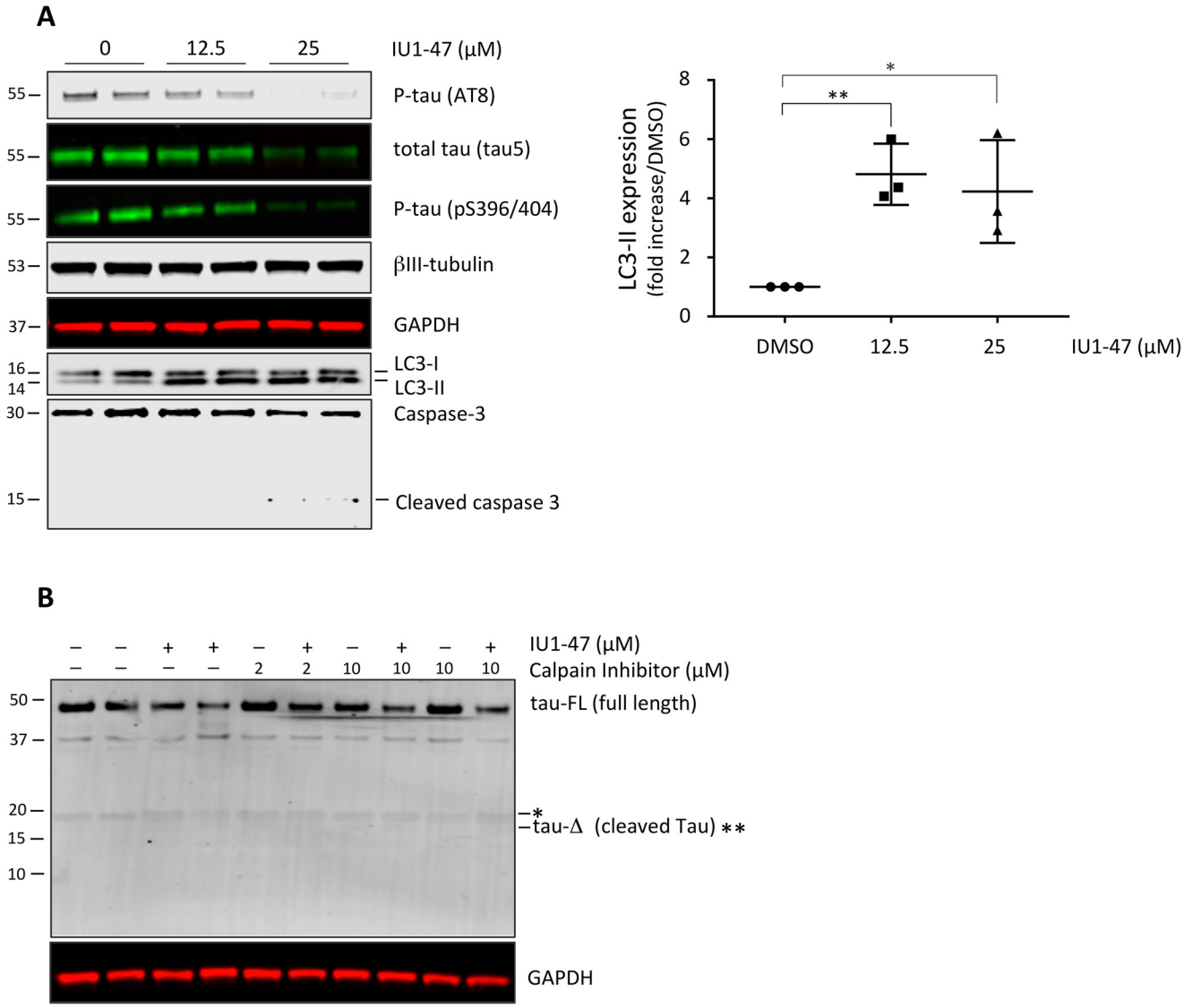

Figure 6. USP14 inhibition elicits an increase in autophagic flux in primary neurons. *A*, rat cortical primary neurons (DIV4) were incubated with graded doses of IU1-47 for 48 h. Cells were harvested, and lysates were prepared and resolved by SDS-PAGE and immunoblotted with antibodies against the LC3, endogenous total tau (tau5), multiple forms of phosphorylated (*P*) tau (pSer-396/404 and pSer-202/pThr-205), and caspase-3 (full-length and cleaved forms). βIII-tubulin was used as a marker for structural integrity. GAPDH was used as a loading control. Proteins of interest were visualized with IRDye-conjugated secondary antibodies using an Odyssey imaging system. A representative sample of three independent experiments is shown. The *right panel* shows the quantification of LC3-II expression. Each data point represents the average from two independent samples. *Error bars* represent S.D. from $n = 3$ independent experiments. *Asterisks* denote p values <0.05; *double asterisks* denote p values <0.01 of differences from appropriate DMSO controls (one-way ANOVA, Tukey–Kramer post hoc analyses). The images were produced from three independent gels to avoid stripping the membrane. *B*, rat cortical primary neurons (DIV3) were treated with 12.5 μM IU1-47 for 48 h in combination with the calpain inhibitor calpeptin (2 and 10 μM). Lysates were prepared, and proteins were resolved by SDS-PAGE followed by immunoblot analysis using monoclonal tau antibody (amino acids 210–241; clone tau5) to detect full-length tau (*tau-FL*) and, if present, the 17-kDa tau fragment resulting from calpain-mediated tau cleavage (*one asterisk* denotes an unspecific band; *two asterisks* denotes the expected 17-kDa fragment position in the blot above). GAPDH was used as a loading control. The blot above is representative of two independent experiments.

To better probe USP14 function in cells, we have developed a significantly improved derivative of IU1. The new compound, IU1-47, is 10-fold more potent. IU1-47 should prove to be an effective research tool. The improved properties of this compound may facilitate the identification of new functions of USP14 while helping to minimize off-target effects.

IU1-47 potentiates endogenous protein degradation in cultured neurons

Previous work showed that IU1 can be effective in lowering tau levels in transiently transfected MEF cells, although the translatability of this model system into a more physiological context was uncertain (8). We therefore set out in this study to examine whether the influence of USP14 inhibition on tau levels was achievable in neurons; whether tau overexpression, as previously used, was necessary for the effect; whether mutant forms of tau associated with disease were affected by USP14 inhibition; and whether dosing regimes could be found in which tau levels were reduced without substantial effects on neuronal viability. It will be important to confirm that USP14 inhibitors can promote phosphotau clearance in not only primary neurons but also in animal models. Studies in animals will be facilitated by further improvement in the properties of these compounds.

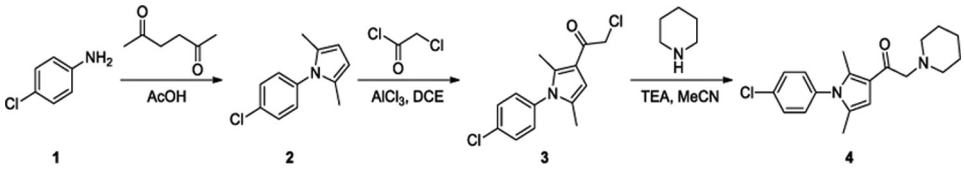

Scheme 1

IU1-47 and phosphotau elimination

We show here by quantitative immunoblot analysis as well as mass spectrometry that IU1-47 induces tau degradation in cultured primary neurons derived from either the cortex or hippocampus. IU1-47 treatment reduces the levels of both total and phosphotau isoforms as shown by monitoring the differential decrease of several phosphotau epitopes that are associated with AD pathology. Specifically, Ser-202/Thr-205 and Ser-396/404, the predominant tau phosphorylation sites in later stages of AD, are attenuated upon treatment. IU1-47 can similarly target pathological tau species such as the P301L and P301S mutants. P301L lies within the microtubule-binding domain of tau, and the substitution may impair tau binding to microtubules and promote its hyperphosphorylation, resulting in a toxic gain of function (71, 72). The htau-A152T variant is less extensively characterized but may be linked to an elevated incidence of FTD spectrum and AD diseases (46, 73–76). The degradation of both total and some phosphotau species might reflect the fact that phosphorylated tau binds less efficiently to microtubules (77, 78). If not bound to microtubules, tau may assume a conformation that is selectively recognized by a ubiquitin ligase or simply be more accessible to either a ligase or the proteasome. Alternatively, tau may be ubiquitinated by a phosphoepitope-specific ligase.

Lys-174 mediates the IU1-47 effect on tau degradation

Recent studies have implicated acetylation in tau-mediated neurodegeneration (35, 50). In particular, Lys-174 has been shown to play a key role in this process, and there is evidence that Lys-174 acetylation occurs at very early Braak stages in AD patients. Lys-174 also been shown to be required for proteasome-mediated degradation, perhaps because it is a ubiquitination site (50). We show here that the tau-K174Q mutant did not respond to the IU1-47 treatments in primary neurons. These results point to the specificity of the IU1-47 effect on tau turnover.

USP14 and autophagy

Recent studies have shown that inhibition of USP14 activity by IU1 (10) induces autophagic flux in H4 cells. Accordingly, deletion of the *Usp14* gene increases bulk turnover through both the autophagy and proteasome pathways (26). Autophagy is of particular importance to maintain homeostasis in nondividing cells such as neurons (79), and it has become increasingly clear that autophagy plays a major role in the aging brain and in neurodegeneration (80). Consistently, neurodegeneration mouse models have shown amelioration after treatment with autophagy-stimulating agents (81). We show here that, in addition to stimulating the degradation of proteasome substrates, IU1-47 also stimulates autophagy in neuronal cells. This additional effect of IU1-47 suggests that USP14 is an important regulator of two key mechanisms responsible for maintaining proteostasis in neuronal cells: autophagy and the ubiquitin-proteasome system.

Suppression of the UPS has proven to be an effective strategy in the treatment of multiple myeloma with proteasome inhibitors in widespread clinical use (82). However, enhancing the UPS might also be a useful therapeutic strategy given the existence of numerous proteopathies characterized by the expression of toxic proteins. Among the straightforward approaches to enhancing UPS output is the suppression of negative regulators and particularly deubiquitinating enzymes. The feasibility of approaches of this type will be critically dependent on the substrates of the DUB in question. In the case of USP14, we found that lowering of a key disease-associated target can be achieved in all cell types tested, including neurons generated from human-derived iPSCs (Figs. 3 and 4 and supplemental Fig. 7). Future studies will determine the extent to which small-molecule inhibitors of USP14 can elicit broader cytoprotective effects both in cell culture and *in vivo* (17, 18).

To evaluate the cellular effects of USP14 inhibition more globally, it will be important to identify additional substrates of USP14 through proteomics and to further improve the potency and selectivity of USP14 inhibitors. Such studies are currently underway.

Experimental procedures

Synthesis of IU1-47

Compound IU1-47, *i.e.* 1-(1-(4-chlorophenyl)-2,5-dimethyl-*1H*-pyrrol-3-yl)-2-(piperidin-1-yl)ethanone (compound 4), was synthesized by Sundia Meditech (Shanghai, China) according to Scheme 1.

Synthesis of compound 2

A mixture of 4-chloroaniline 1 (7.65 g; 60.0 mmol) and hexane-2,5-dione (34.2 g; 300.0 mmol) in acetic acid (40 ml) was heated at 100 °C for 1 h. The solvent was then evaporated, and the residue was purified by silica column chromatography to afford the title compound (11.07 g; yield, 89.8%).

Synthesis of compound 3

2-Chloroacetyl chloride (6.78 g; 60.0 mmol) was added to a suspension of $AlCl_3$ (7.98 g; 60.0 mmol) in 1,2-dichloroethane (50 ml) at 0 °C. The resulting mixture was stirred for 30 min and was then added to a solution of compound 2 (6.17 g; 30.0 mmol) in 1,2-dichloroethane (50 ml) at 0 °C. The reaction mixture was then allowed to warm to room temperature and stirred for 2 h. The mixture was poured into ice-water (20 ml) and extracted with dichloromethane (3 × 15 ml). The combined organic layers were dried over $MgSO_4$, filtered, and concentrated *in vacuo*.

The residue was purified by silica gel chromatography to afford the title compound (3.37 g; yield, 39.9%).

Synthesis of compound 4 (IU1-47)

Piperidine (28 mg; 0.33 mmol) was added to a solution of compound 3 (85 mg; 0.3 mmol) and triethylamine (61 mg; 0.6 mmol) in acetonitrile (10 ml). After being heated at reflux for 1 h, the mixture was concentrated. The residue was redissolved in dichloromethane (30 ml), washed with saturated aqueous $NaHCO_3$ (10 ml), dried over $MgSO_4$, concentrated *in vacuo*, and purified by silica gel chromatography to afford the title compound (83 mg; yield, 83.8%). ^{1}H NMR (400 MHz, DMSO-d_6) of IU1-47 showed: δ 7.64 (d, $J = 8.8$ Hz, 2H), 7.39 (d, $J = 8.8$ Hz, 2H), 6.50 (s, 1H), 3.43 (s, 2H), 2.50–2.40 (m, 4H), 2.23 (s, 3H), 1.95 (s, 3H), 1.55–1.45 (m, 4H), 1.43–1.35 (m, 2H) (supplemental Fig. 1). LC-MS ($M + H^+$) m/z was calculated to be 331.2; the experimental value was 331.1 (supplemental Fig. 2).

LC-MS analysis of IU1-47

Stability in the presence of USP14—IU1-47 was incubated at 2 μM in the presence or absence of 2 μM recombinant human USP14. Proteasome was then added at 0.5 μM to activate USP14. After 50 min at room temperature, the reaction mixture was applied to an LC-MS analytical system (Agilent series 1200LC/6130MS) with a reverse-phase pentafluorophenyl column (Phenomenex Luna, 100 × 4.60 mm, 5 μm) and a gradient solvent system (from 10 to 100% CH_3CN in 0.1% formic acid) over 11 min. 20 μl of sample were injected for each analysis. The collected LC-MS profiles were further analyzed by extracting specific ions of m/z at 331 for IU1-47 in the positive-ion MS mode. IU1-47 was eluted at ~8.0 min (supplemental Fig. 3).

Dissolving and storing IU1-47—Anhydrous DMSO (high quality DMSO is critical for proper solubilization) was used to dissolve IU1-47. Powdered IU1-47 was dissolved in 100% DMSO at ~25 mM, and the sample was heated at 60 °C for 6 min. This brief heat treatment does not result in detectable decomposition of the compound as monitored by LC-MS. The compound was stored at −80 °C or in liquid nitrogen; freeze-thaw cycles were avoided. The main consideration in working with the compound is to avoid its precipitation, which may occur at high concentrations in tissue culture, during thawing if done slowly, or when some dilution schemes are used. Thawing was performed at 37 °C. Typically, IU1-47 was added to the different culture media directly from the 25 mM stock. It is recommended to quickly confirm that cultures are free of precipitated IU1-47 using a light microscope at 10× magnification.

In vitro biochemical assays, biochemical reagents, and antibodies

Human 26S proteasome and recombinant USP14 were affinity-purified as described previously (8). Ubiquitin, Ub-AMC, and ubiquitin vinyl sulfone were purchased from R&D Systems (U-100H, U-550, and U-202, respectively). IU1 derivatives were dissolved in anhydrous DMSO (276855, Sigma) as described above and stored at −80 °C in aliquots. Freeze-thaw cycles were avoided. The plasmid expressing tau was kindly provided by V. M. Lee (University of Pennsylvania). Ubiquitinated Sic1^{PY} and ubiquitinated N-terminal cyclin B1 were prepared essentially as described (8, 39). Calpeptin (C8999, Sigma) was reconstituted in DMSO according to the manufacturer's protocol.

Staurosporine was used as described (83, 84) (S6942, Sigma). Sources of commercial antibodies were as follows: anti-T7-HRP (69048-3, EMD Millipore); anti-HA-HRP (3F10) (120113819001, Roche Applied Science); anti-tau (tau5) (AHB0042, Life Technologies); anti-actin (A5060, Sigma); anti-GAPDH (6C5) (ab8245, Abcam); anti-GAPDH (G9545, Sigma); anti-USP14 (A300-920A, Bethyl Laboratories); anti-tau1 (PC1C6) (MAB3420, EMD Millipore); anti-phosphotau (AT8) (MN1020, Thermo Scientific); tau pSer-396 (44752G, Life Technologies); anti-tubulin β-III (1967-1, Epitomics); anti-LC3B (NB100-2220SS, Novus Biologicals); anti-caspase-3 (9662, Cell Signaling Technology); anti-tau (MAB361, Millipore); and anti-CP-13, anti-CP-27, and anti-PHF1 phosphotau antibodies (kind gifts from P. Davies, Albert Einstein School of Medicine, New York). IRDye-conjugated secondary antibodies were from LI-COR Biosciences (926-32212, 926-68020, 926-68073, and 926-32213).

Ub-AMC hydrolysis assay

To measure the USP14 enzymatic activity, 30 nM recombinant USP14 was reconstituted with 2.5 nM ubiquitin vinyl sulfone-treated human proteasomes (8) in the presence of graded concentrations of each IU1 derivative. The reaction mixture was prepared in Ub-AMC assay buffer (50 mM Tris-HCl (pH 7.5), 1 mM EDTA, 1 mM ATP, 5 mM $MgCl_2$, 1 mM DTT, and 1 mg/ml ovalbumin). Ub-AMC was added to a final concentration of 1 μM to initiate the reaction, and its cleavage was monitored in real time by measuring fluorescence at an excitation of 365 nm and an emission of 460 nm with an Envision plate reader (model 2103, PerkinElmer Life Sciences) equipped with an appropriate mirror (*e.g.* LANCE/DELFIA, 400 nm). To test the specificity of USP14 inhibitors, each IU1 derivative was also tested against 1.5 nM human IsoT/USP5 in parallel. Free ubiquitin (0.01–0.02 μM) was added to activate IsoT/USP5 in the reaction (8). For measuring IC_{50} values, dose-response curves were obtained with percent inhibition for each inhibitor being plotted. Curve fitting was performed using graphic analysis software (GraphPad Prism and SigmaPlot).

In vitro ubiquitin conjugate degradation and deubiquitination assays

Human proteasomes (4 nM) were incubated with polyubiquitinated N-terminal cyclin B1 (Ub_n-NCB1; ~120 nM final; HA-tagged) or polyubiquitinated Sic1^{PY} (WT or K63R Ub_n-Sic1^{PY}; ~240 nM final; T7-tagged) in proteasome assay buffer (50 mM Tris-HCl (pH 7.5), 5 mM $MgCl_2$, and 5 mM ATP or 5 mM ADP for proteasome purified in the presence of ADP). N-terminally His-tagged human USP14 was expressed from the plasmid pET15b-USP14 (a generous gift from G. Tian) and purified using nickel-nitrilotriacetic acid-agarose resin (30210, Qiagen) according to the manufacturer's instructions. Purified recombinant USP14, where indicated, was reconstituted with proteasome for 5 min before initiating the deubiquitination reaction. To test IU1-47, the compound was preincubated at 17 μM with USP14 for 5 min before adding proteasome. Reactions were quenched by adding 5× SDS-PAGE sample buffer, boiled for 5

min, and then subjected to SDS-PAGE and immunoblot analysis using anti-HA-HRP or anti-T7-HRP antibody.

Transient expression of tau in MEFs

Usp14$^{-/-}$ and wild-type MEFs were described previously (11). Wild-type and *Usp14*$^{-/-}$ murine embryonic fibroblasts were transfected with Metafectene-Pro (Biontex) in 12-well plates according to the manufacturer's protocol. Forty-eight hours after transfection with 1 μg of human tau pcDNA3.1 DNA, cells were treated with IU1-47 (0, 20, 30, 40, or 50 μM) by exchanging the medium (DMEM + FBS) with prewarmed medium containing IU1-47 and then incubated for 9 h. Cells were harvested by scraping in the presence of PBS. Cells were then spun at 1,900 $\times$ *g* for 4 min at room temperature. The cell pellets were frozen overnight at −80 °C prior to immunoblot analysis. Cell lysates were prepared using buffer A (8 M urea, 75 mM NaCl, 50 mM HEPES-NaOH (pH 8.2), 1 mM NaF, 1 mM β-glycerophosphate, 1 mM Na_3VO_4, 10 mM sodium pyrophosphate, 1 mM PMSF, and protease inhibitor mixture (11836170001, Roche Applied Science)). For immunoblotting, 10 μg of protein were used.

Primary neuronal cultures

Murine primary neuronal cultures were established from either cortex or hippocampus of C57BL/6N mouse embryos (E16; originating from Charles River Laboratories and a kind gift of the M. Greenberg laboratory). Purified cells were plated at 2 $\times$ 10^6 cells/well onto 6-well plates coated with poly-D-lysine in Neurobasal medium (21103-049, Life Technologies) supplemented with serum-free B27 (17504-044, Thermo Scientific) and GlutaMAX (35050-079, Thermo Scientific). After ~3 h, the medium was removed, and new Neurobasal medium supplemented with serum-free B27 and GlutaMAX was added to the cells. All treatments were performed at 4–6 DIV in Neurobasal medium supplemented with either serum-free B27 or N2 supplement (17502-048, Life Technologies). Rat primary neuronal cultures were established from either the cortex or hippocampus of Long–Evans rats (E18; originating from Charles River Laboratories and a kind gift from the Sahin laboratory, Boston Children's Hospital). These cells were cultured under the same conditions as their murine counterparts (see above).

Infection of primary neuronal cultures with AAV

Rat primary neuronal cultures were established as described above. All experiments were performed at 4–6 DIV in Neurobasal medium supplemented with B27 unless noted otherwise. The AAV transfer vectors AAV1-CBA-tau-A152T-WPRE-BGH-poly(A), CBA-tau-P301S-WPRE-BGH-poly(A), and AAV1-CBA-wild-type-tau-WPRE-BGH-poly(A) were generated and purified by GeneDetect (Sarasota, FL).

IU1-47 treatment of primary neurons

IU1-47 treatments were performed by replacing the culture medium with fresh prewarmed medium containing IU1-47. Treatments lasted 48 h unless otherwise indicated. Cotreatment with the calpain inhibitor calpeptin was done under the same conditions used for IU1-47.

Immunoblot analysis of primary neurons

Cells were lysed and harvested as described above. Lysates were then centrifuged at 14,000 $\times$ *g* at 4 °C for 10 min. Supernatants were collected, and protein concentrations were measured using a standard BCA assay (23227, Pierce). Analysis was carried out using IRDye680 and -800 infrared dye-conjugated secondary antibodies for quantitative immunoblotting using an Odyssey infrared imaging system (LI-COR Biosciences). Immunoblot bands were quantified using Odyssey software (LI-COR Biosciences).

Statistical analysis of quantitative immunoblotting

Data are presented as means ± S.D. unless otherwise indicated. Statistical analysis was performed with GraphPad Prism. Differences among multiple (≥3) means with one variable were evaluated by one-way ANOVA and the Bonferroni post hoc test unless otherwise indicated. Differences between two means were assessed with the unpaired two-tailed *t* test. $p < 0.05$ was considered significant.

Mass spectrometry AQUA

Cell lysates were prepared using buffer A. Subsequently, cysteines were reduced with 5 mM DTT (for 25 min at 56 °C) and alkylated with 14 mM iodoacetamide (for 30 min at room temperature). A 10-μg aliquot of protein from each sample was diluted to 1 M urea with 50 mM HEPES-NaOH (pH 8.5) and digested overnight at 37 °C with 10 ng/μl Lys-C (125-02543, Wako). Just before digestion, heavy isotope-labeled synthetic peptide (Pierce) was spiked into the samples (peptide sequence, SSAKSRLQTAPVPMPD*L*K; heavy Leu, +7 Da). After digestion, peptides were acidified to a final concentration of 5% formic acid, desalted using homemade stage tips as described previously (85), and lyophilized. Dried peptides were resuspended in a solution of 5% formic acid and 0.01% H_2O_2 (final concentrations), incubated for 30 min at room temperature, and then analyzed by mass spectrometry. Quantitative LC-MS analysis was performed on an Exactive-Orbitrap mass spectrometer equipped with a Thermo Fisher nanospray source, a PAL HTC autosampler for sample handling, and an Accela HPLC pump for liquid chromatography separation. Skyline (86) software was used to perform MS1 AQUA analysis.

RNA isolation and quantitative PCR

Primary neuronal cultures were established from murine hippocampi and treated with IU1-47 for 48 h. They were scraped with 1× PBS, spun down at 1,900 $\times$ *g* for 4 min, and subsequently stored at −80 °C. RNA isolation was performed using the RNeasy Mini kit (74104, Qiagen) according to the manufacturer's instructions. Quantitative PCR was performed using an ABI Prism 7900HT detection system (Life Technologies) according to the manufacturer's protocol. The TaqMan gene expression assays used were: MAPT (Mm00521988, Life Technologies) and 18S (Hs03003631, Life Technologies). Analysis was performed using the comparative C_T method (87).

Mouse strains used in this study

Primary neurons were isolated from the following mouse strains: 5XFAD (The Jackson Laboratory stock number

006554), 3XFAD (The Jackson Laboratory stock number 034830), and C57BL/6N for wild-type mice.

Human induced pluripotent stem cell neuron generation and IU1-47 treatment

Generation of an expandable neural progenitor cell line (NPC; 8330-8) through an iPSC intermediate from human fibroblasts (GM8330, Corielle Institute) was previously described (88). The resulting NPC was terminally differentiated into neurons by plating at a density of 8×10^5 cells/well using a 6-well cell culture plate (precoated with 20 μg/ml polyornithine (Sigma) and 5 μg/ml laminin (Sigma) in PBS overnight at 37 °C) in neural medium (consisting of 70% DMEM (high glucose 1×; Gibco catalog number 11995), 30% Ham's F-12 with L-glutamine (Corning Cellgro), B27 (Gibco), and penicillin/streptomycin (Gibco). The cells were fed twice weekly for 6 weeks by replacement of half of the neural media in each well. By 10 days of neural differentiation, the cells were immunopositive for the neuronal marker βIII-tubulin (TUJ1) and had generated axonal (SMI312-positive) and dendritic (MAP2-positive) neuronal processes (88).

IU1-47 treatment started at week 6 of differentiation for 96 h, the first dose was applied at $t = 0$, and the second dose was applied 2 days later. Cells were harvested by scraping in the presence of PBS. Cells were then spun at 1,300 × *g* for 5 min at room temperature. Cell pellets were frozen overnight at −80 °C prior to immunoblot analysis. Cell lysates were prepared using buffer A. For immunoblotting, 10 μg of protein were used.

Primary antibodies and other reagents in Figs. 3A and 5

The following reagents were purchased from the indicated companies: tau5 antibody (Bio-Source), GAPDH antibody (Sigma), and anti-HA (Cell Signaling Technology). MG-132 was purchased from EMD Millipore.

Primary neuronal cultures and lentiviral infections in Figs. 3A and 5

Primary cultures were established from cortices of Sprague-Dawley rat pups (Charles River Laboratories) on postnatal day 0 or 1. Purified cells were plated at 160,000 cells/ml in Neurobasal medium supplemented with B27 (Thermo Scientific) on poly-ornithine-coated plates. All treatments were performed at 7–13 DIV in Neurobasal medium supplemented with N2 (Thermo Fisher Scientific) unless noted otherwise.

Lentivirus was generated, purified, and used for infection as described (89). Recombinant lentivirus was produced by cotransfection of the shuttle vector, two helper plasmids, delta8.9 packaging vector, and vesicular stomatitis virus G envelope vector into 293T cells and purified by ultracentrifugation. Viral titers were measured by p24 enzyme-linked immunosorbent assays at the Gladstone-University of California San Francisco Laboratory of Clinical Virology.

IU1-47/MG-132 treatment of neurons

Rat primary neuronal cultures at DIV9–12 were treated with IU1-47 (25 μM) and MG-132 (10 μM) for 48 h.

In vivo ubiquitination assays

Procedures were modified from a published study (35). HEK293T cells were transfected with expression vectors encoding FLAG-tagged human WT tau or mutant tau and HA-ubiquitin. After 24-h incubation, cells were treated with IU1-47 (10 μM) in Dulbecco's modified Eagle's medium and incubated for 20 h. MG-132 (20 μM) was then added and incubated for 4 h. Cells were lysed in ubiquitination buffer (20 mM Tris-HCl (pH 7.5), 0.1 mM EDTA, 0.2% Triton X-100, 150 mM NaCl, and protease inhibitor mixture). Supernatant proteins were immunoprecipitated with FLAG M2-agarose beads (Sigma) for 3 h at 4 °C. Reactions were washed at least three times with ubiquitination buffer and analyzed by SDS-PAGE and Western blotting with anti-HA antibody.

Author contributions—B.-H. L. performed all the initial characterization of the compound and all *in vitro* experiments. M. B. performed the IU1-47 experiments in mouse and rat primary neurons. J. R. performed experiments in rat primary neurons. M. A. P. performed the AQUA analysis shown in Fig. 3*C* and the experiment shown in supplemental Fig. 5. S.-W. M. and L. G. generated results shown in Fig. 5. C. S. assisted in the analysis shown in supplemental Fig. 3. S. E. purified Sic1PY-related reagents and prepared ubiquitinated Sic1PY. C. C. and M. C. S. generated the human iPSCs. M. B., C. C., and M. C. S. generated the iPSC data. K. M. H. provided technical assistance. T. C. G. together with R. W. K. designed synthesis methods for the SAR analysis of IU1 and oversaw quality control of these compounds. S. J. H., S. P. G., R. W. K., and D. F. were responsible for overall design and oversight of the project. D. F., M. B., and B.-H. L. wrote the manuscript.

Acknowledgments—We gratefully acknowledge the M. Greenberg laboratory (Harvard Medical School) and the M. Sahin laboratory (Boston Children's Hospital) for mouse and rat primary neurons, respectively. We thank A. Amon (Massachusetts Institute of Technology), A. M. Cuervo (Albert Einstein School of Medicine, New York), P. Davies (Albert Einstein School of Medicine, New York), V. Lee (University of Pennsylvania), and G. Tian (Harvard Medical School) for reagents. We also thank J. Hanna, S. Hung, and A. Nguyen for critical reading of the manuscript.

References

1. Budenholzer, L., Cheng, C. L., Li, Y., and Hochstrasser, M. (2017) Proteasome structure and assembly. *J. Mol. Biol.* **427,** 3500–3524
2. Finley, D. (2009) Recognition and processing of ubiquitin-protein conjugates by the proteasome. *Annu. Rev. Biochem.* **78,** 477–513
3. Collins, G. A., and Goldberg, A. L. (2017) The logic of the 26S proteasome. *Cell* **169,** 792–806
4. Inobe, T., and Matouschek, A. (2014) Paradigms of protein degradation by the proteasome. *Curr. Opin. Struct. Biol.* **24,** 156–164
5. Goldberg, A. L. (2007) Functions of the proteasome: from protein degradation and immune surveillance to cancer therapy. *Biochem. Soc. Trans.* **35,** 12–17
6. Matyskiela, M. E., and Martin, A. (2013) Design principles of a universal protein degradation machine. *J. Mol. Biol.* **425,** 199–213
7. Leggett, D. S., Hanna, J., Borodovsky, A., Crosas, B., Schmidt, M., Baker, R. T., Walz, T., Ploegh, H., and Finley, D. (2002) Multiple associated proteins regulate proteasome structure and function. *Mol. Cell* **10,** 495–507
8. Lee, B.-H., Lee, M. J., Park, S., Oh, D.-C., Elsasser, S., Chen, P.-C., Gartner, C., Dimova, N., Hanna, J., Gygi, S. P., Wilson, S. M., King, R. W., and Finley,

D. (2010) Enhancement of proteasome activity by a small-molecule inhibitor of USP14. *Nature* **467,** 179–184
9. Hanna, J., Hathaway, N. A., Tone, Y., Crosas, B., Elsasser, S., Kirkpatrick, D. S., Leggett, D. S., Gygi, S. P., King, R. W., and Finley, D. (2006) Deubiquitinating enzyme Ubp6 functions noncatalytically to delay proteasomal degradation. *Cell* **127,** 99–111
10. Xu, D., Shan, B., Sun, H., Xiao, J., Zhu, K., Xie, X., Li, X., Liang, W., Lu, X., Qian, L., and Yuan, J. (2016) USP14 regulates autophagy by suppressing K63 ubiquitination of Beclin 1. *Genes Dev.* **30,** 1718–1730
11. Crimmins, S., Jin, Y., Wheeler, C., Huffman, A. K., Chapman, C., Dobrunz, L. E., Levey, A., Roth, K. A., Wilson, J. A., and Wilson, S. M. (2006) Transgenic rescue of ataxia mice with neuronal-specific expression of ubiquitin-specific protease 14. *J. Neurosci.* **26,** 11423–11431
12. Wilson, S. M., Bhattacharyya, B., Rachel, R. A., Coppola, V., Tessarollo, L., Householder, D. B., Fletcher, C. F., Miller, R. J., Copeland, N. G., and Jenkins, N. A. (2002) Synaptic defects in ataxia mice result from a mutation in Usp14, encoding a ubiquitin-specific protease. *Nat. Genet.* **32,** 420–425
13. Vaden, J. H., Bhattacharyya, B. J., Chen, P.-C., Watson, J. A., Marshall, A. G., Phillips, S. E., Wilson, J. A., King, G. D., Miller, R. J., and Wilson, S. M. (2015) Ubiquitin-specific protease 14 regulates c-Jun N-terminal kinase signaling at the neuromuscular junction. *Mol. Neurodegener.* **10,** 3
14. Marshall, A. G., Watson, J. A., Hallengren, J. J., Walters, B. J., Dobrunz, L. E., Francillon, L., Wilson, J. A., Phillips, S. E., and Wilson, S. M. (2013) Genetic background alters the severity and onset of neuromuscular disease caused by the loss of ubiquitin-specific protease 14 (usp14). *PLoS One* **8,** e84042
15. Hanna, J., Meides, A., Zhang, D. P., and Finley, D. (2007) A ubiquitin stress response induces altered proteasome composition. *Cell* **129,** 747–759
16. Walters, B. J., Hallengren, J. J., Theile, C. S., Ploegh, H. L., Wilson, S. M., and Dobrunz, L. E. (2014) A catalytic independent function of the deubiquitinating enzyme USP14 regulates hippocampal synaptic short-term plasticity and vesicle number. *J. Physiol.* **592,** 571–586
17. Sareen-Khanna, K., Papillon, J., Wing, S. S., and Cybulsky, A. V. (2016) Role of the deubiquitinating enzyme ubiquitin-specific protease-14 in proteostasis in renal cells. *Am. J. Physiol. Renal Physiol.* **311,** F1035–F1046
18. Min, J.-W., Lü, L., Freeling, J. L., Martin, D. S., and Wang, H. (2017) USP14 inhibitor attenuates cerebral ischemia/reperfusion-induced neuronal injury in mice. *J. Neurochem.* **140,** 826–833
19. Lee, B.-H., Lu, Y., Prado, M. A., Shi, Y., Tian, G., Sun, S., Elsasser, S., Gygi, S. P., King, R. W., and Finley, D. (2016) USP14 deubiquitinates proteasome-bound substrates that are ubiquitinated at multiple sites. *Nature* **532,** 398–401
20. Homma, T., Ishibashi, D., Nakagaki, T., Fuse, T., Mori, T., Satoh, K., Atarashi, R., and Nishida, N. (2015) Ubiquitin-specific protease 14 modulates degradation of cellular prion protein. *Sci. Rep.* **5,** 11028
21. McKinnon, C., Goold, R., Andre, R., Devoy, A., Ortega, Z., Moonga, J., Linehan, J. M., Brandner, S., Lucas, J. J., Collinge, J., and Tabrizi, S. J. (2016) Prion-mediated neurodegeneration is associated with early impairment of the ubiquitin-proteasome system. *Acta Neuropathol.* **131,** 411–425
22. Liao, Y., Liu, N., Hua, X., Cai, J., Xia, X., Wang, X., Huang, H., and Liu, J. (2017) Proteasome-associated deubiquitinase ubiquitin-specific protease 14 regulates prostate cancer proliferation by deubiquitinating and stabilizing androgen receptor. *Cell Death Dis.* **8,** e2585
23. Zhu, Y., Zhang, Y., Sui, Z., Zhang, Y., Liu, M., and Tang, H. (2017) USP14 de-ubiquitinates vimentin and miR-320a modulates USP14 and vimentin to contribute to malignancy in gastric cancer cells. *Oncotarget* **8,** 48725–48736
24. Chen, M., Meng, Q., Qin, Y., Liang, P., Tan, P., He, L., Zhou, Y., Chen, Y., Huang, J., Wang, R.-F., and Cui, J. (2016) TRIM14 inhibits cGAS degradation mediated by selective autophagy receptor p62 to promote innate immune responses. *Mol. Cell* **64,** 105–119
25. Nakashima, A., Ohnuma, S., Kodani, Y., Kaneko, Y. S., Nagasaki, H., Nagatsu, T., and Ota, A. (2016) Inhibition of deubiquitinating activity of USP14 decreases tyrosine hydroxylase phosphorylated at Ser19 in PC12D cells. *Biochem. Biophys. Res. Commun.* **472,** 598–602
26. Kim, H. T., and Goldberg, A. L. (2017) The deubiquitinating enzyme Usp14 allosterically inhibits multiple proteasomal activities and ubiquitin-independent proteolysis. *J. Biol. Chem.* **292,** 9830–9839
27. Hu, M., Li, P., Song, L., Jeffrey, P. D., Chenova, T. A., Wilkinson, K. D., Cohen, R. E., and Shi, Y. (2005) Structure and mechanisms of the proteasome-associated deubiquitinating enzyme USP14. *EMBO J.* **24,** 3747–3756
28. Jung, H., Kim, B.-G., Han, W. H., Lee, J. H., Cho, J.-Y., Park, W. S., Maurice, M. M., Han, J.-K., Lee, M. J., Finley, D., and Jho, E.-H. (2013) Deubiquitination of Dishevelled by Usp14 is required for Wnt signaling. *Oncogenesis* **2,** e64
29. Hjerpe, R., Bett, J. S., Keuss, M. J., Solovyova, A., McWilliams, T. G., Johnson, C., Sahu, I., Varghese, J., Wood, N., Wightman, M., Osborne, G., Bates, G. P., Glickman, M. H., Trost, M., Knebel, A., *et al.* (2016) UBQLN2 mediates autophagy-independent protein aggregate clearance by the proteasome. *Cell* **166,** 935–949
30. Kabashi, E., and Durham, H. D. (2006) Failure of protein quality control in amyotrophic lateral sclerosis. *Biochim. Biophys. Acta* **1762,** 1038–1050
31. Myeku, N., Clelland, C. L., Emrani, S., Kukushkin, N. V., Yu, W. H., Goldberg, A. L., and Duff, K. E. (2016) Tau-driven 26S proteasome impairment and cognitive dysfunction can be prevented early in disease by activating cAMP-PKA signaling. *Nat. Med.* **22,** 46–53
32. Lokireddy, S., Kukushkin, N. V., and Goldberg, A. L. (2015) cAMP-induced phosphorylation of 26S proteasomes on Rpn6/PSMD11 enhances their activity and the degradation of misfolded proteins. *Proc. Natl. Acad. Sci. U.S.A.* **112,** E7176–E7185
33. Rademakers, R., Cruts, M., and van Broeckhoven, C. (2004) The role of tau (MAPT) in frontotemporal dementia and related tauopathies. *Hum. Mutat.* **24,** 277–295
34. Sanders, D. W., Kaufman, S. K., DeVos, S. L., Sharma, A. M., Mirbaha, H., Li, A., Barker, S. J., Foley, A. C., Thorpe, J. R., Serpell, L. C., Miller, T. M., Grinberg, L. T., Seeley, W. W., and Diamond, M. I. (2014) Distinct tau prion strains propagate in cells and mice and define different tauopathies. *Neuron* **82,** 1271–1288
35. Min, S.-W., Cho, S.-H., Zhou, Y., Schroeder, S., Haroutunian, V., Seeley, W. W., Huang, E. J., Shen, Y., Masliah, E., Mukherjee, C., Meyers, D., Cole, P. A., Ott, M., and Gan, L. (2010) Acetylation of tau inhibits its degradation and contributes to tauopathy. *Neuron* **67,** 953–966
36. Irwin, D. J., Cohen, T. J., Grossman, M., Arnold, S. E., McCarty-Wood, E., Van Deerlin, V. M., Lee, V. M., and Trojanowski, J. Q. (2013) Acetylated tau neuropathology in sporadic and hereditary tauopathies. *Am. J. Pathol.* **183,** 344–351
37. Santacruz, K., Lewis, J., Spires, T., Paulson, J., Kotilinek, L., Ingelsson, M., Guimaraes, A., DeTure, M., Ramsden, M., McGowan, E., Forster, C., Yue, M., Orne, J., Janus, C., Mariash, A., *et al.* (2005) Tau suppression in a neurodegenerative mouse model improves memory function. *Science* **309,** 476–481
38. Young, Z. T., Mok, S. A., and Gestwicki, J. E. (2017) Therapeutic strategies for restoring tau homeostasis. *Cold Spring Harb. Perspect. Med.* 10.1101/cshperspect.a024612
39. Saeki, Y., Isono, E., and Toh-E, A. (2005) Preparation of ubiquitinated substrates by the PY motif-insertion method for monitoring 26S proteasome activity. *Methods Enzymol.* **399,** 215–227
40. Gendron, T. F., and Petrucelli, L. (2009) The role of tau in neurodegeneration. *Mol. Neurodegener.* **4,** 13
41. Götz, J., Probst, A., Spillantini, M. G., Schäfer, T., Jakes, R., Bürki, K., and Goedert, M. (1995) Somatodendritic localization and hyperphosphorylation of tau protein in transgenic mice expressing the longest human brain tau isoform. *EMBO J.* **14,** 1304–1313
42. Morris, M., Maeda, S., Vossel, K., and Mucke, L. (2011) The many faces of tau. *Neuron* **70,** 410–426
43. Augustinack, J. C., Schneider, A., Mandelkow, E.-M., and Hyman, B. T. (2002) Specific tau phosphorylation sites correlate with severity of neuronal cytopathology in Alzheimer's disease. *Acta Neuropathol.* **103,** 26–35
44. Sperfeld, A. D., Collatz, M. B., Baier, H., Palmbach, M., Storch, A., Schwarz, J., Tatsch, K., Reske, S., Joosse, M., Heutink, P., and Ludolph, A. C. (1999) FTDP-17: an early-onset phenotype with parkinsonism and epileptic seizures caused by a novel mutation. *Ann. Neurol.* **46,** 708–715

45. Bugiani, O., Murrell, J. R., Giaccone, G., Hasegawa, M., Ghigo, G., Tabaton, M., Morbin, M., Primavera, A., Carella, F., Solaro, C., Grisoli, M., Savoiardo, M., Spillantini, M. G., Tagliavini, F., Goedert, M., *et al.* (1999) Frontotemporal dementia and corticobasal degeneration in a family with a P301S mutation in tau. *J. Neuropathol. Exp. Neurol.* **58,** 667–677
46. Coppola, G., Chinnathambi, S., Lee, J. J., Dombroski, B. A., Baker, M. C., Soto-Ortolaza, A. I., Lee, S. E., Klein, E., Huang, A. Y., Sears, R., Lane, J. R., Karydas, A. M., Kenet, R. O., Biernat, J., Wang, L.-S., *et al.* (2012) Evidence for a role of the rare p.A152T variant in MAPT in increasing the risk for FTD-spectrum and Alzheimer's diseases. *Hum. Mol. Genet.* **21,** 3500–3512
47. Oddo, S., Caccamo, A., Kitazawa, M., Tseng, B. P., and LaFerla, F. M. (2003) Amyloid deposition precedes tangle formation in a triple transgenic model of Alzheimer's disease. *Neurobiol. Aging* **24,** 1063–1070
48. Vale, C., Alonso, E., Rubiolo, J. A., Vieytes, M. R., LaFerla, F. M., Giménez-Llort, L., and Botana, L. M. (2010) Profile for amyloid-β and tau expression in primary cortical cultures from 3xTg-AD mice. *Cell. Mol. Neurobiol.* **30,** 577–590
49. Oakley, H., Cole, S. L., Logan, S., Maus, E., Shao, P., Craft, J., Guillozet-Bongaarts, A., Ohno, M., Disterhoft, J., Van Eldik, L., Berry, R., and Vassar, R. (2006) Intraneuronal β-amyloid aggregates, neurodegeneration, and neuron loss in transgenic mice with five familial Alzheimer's disease mutations: potential factors in amyloid plaque formation. *J. Neurosci.* **26,** 10129–10140
50. Min, S.-W., Chen, X., Tracy, T. E., Li, Y., Zhou, Y., Wang, C., Shirakawa, K., Minami, S. S., Defensor, E., Mok, S. A., Sohn, P. D., Schilling, B., Cong, X., Ellerby, L., Gibson, B. W., *et al.* (2015) Critical role of acetylation in tau-mediated neurodegeneration and cognitive deficits. *Nat. Med.* **21,** 1154–1162
51. Yang, L. S., and Ksiezak-Reding, H. (1995) Calpain-induced proteolysis of normal human tau and tau associated with paired helical filaments. *Eur. J. Biochem.* **233,** 9–17
52. Hua, Y., and Nair, S. (2015) Proteases in cardiometabolic diseases: pathophysiology, molecular mechanisms and clinical applications. *Biochim. Biophys. Acta* **1852,** 195–208
53. Sorimachi, H., and Ono, Y. (2012) Regulation and physiological roles of the calpain system in muscular disorders. *Cardiovasc. Res.* **96,** 11–22
54. Ferreira, A., and Bigio, E. H. (2011) Calpain-mediated tau cleavage: a mechanism leading to neurodegeneration shared by multiple tauopathies. *Mol. Med.* **17,** 676–685
55. Kiprowska, M. J., Stepanova, A., Todaro, D. R., Galkin, A., Haas, A., Wilson, S. M., and Figueiredo-Pereira, M. E. (2017) Neurotoxic mechanisms by which the USP14 inhibitor IU1 depletes ubiquitinated proteins and tau in rat cerebral cortical neurons: relevance to Alzheimer's disease. *Biochim. Biophys. Acta* **1863,** 1157–1170
56. Brewer, G. J., Torricelli, J. R., Evege, E. K., and Price, P. J. (1993) Optimized survival of hippocampal neurons in B27-supplemented Neurobasal, a new serum-free medium combination. *J. Neurosci. Res.* **35,** 567–576
57. Harrill, J. A., Robinette, B. L., Freudenrich, T. M., and Mundy, W. R. (2015) Media formulation influences chemical effects on neuronal growth and morphology. *In Vitro Cell. Dev. Biol. Anim.* **51,** 612–629
58. King, R. W., and Finley, D. (2014) Sculpting the proteome with small molecules. *Nat. Chem. Biol.* **10,** 870–874
59. Fan, Y.-H., Cheng, J., Vasudevan, S. A., Dou, J., Patel, R. H., Ma, I. T., Rojas, Y., Zhao, Y., Yu, Y., Zhang, H., Shohet, J. M., Nuchtern, J. G., Kim, E. S., and Yang, J. (2013) USP7 inhibitor P22077 inhibits neuroblastoma growth via inducing p53-mediated apoptosis. *Cell Death Dis.* **4,** e867
60. Ponnappan, S., Palmieri, M., Sullivan, D. H., and Ponnappan, U. (2013) Compensatory increase in USP14 activity accompanies impaired proteasomal proteolysis during aging. *Mech. Ageing Dev.* **134,** 53–59
61. Ali, A., Raja, R., Farooqui, S. R., Ahmad, S., and Banerjea, A. C. (2017) USP7 deubiquitinase controls HIV-1 production by stabilizing Tat protein. *Biochem. J.* **474,** 1653–1668
62. Nag, D. K., and Finley, D. (2012) A small-molecule inhibitor of deubiquitinating enzyme USP14 inhibits Dengue virus replication. *Virus Res.* **165,** 103–106
63. Clague, M. J., Barsukov, I., Coulson, J. M., Liu, H., Rigden, D. J., and Urbé, S. (2013) Deubiquitylases from genes to organism. *Physiol. Rev.* **93,** 1289–1315
64. Eletr, Z. M., and Wilkinson, K. D. (2014) Regulation of proteolysis by human deubiquitinating enzymes. *Biochim. Biophys. Acta* **1843,** 114–128
65. Komander, D., and Rape, M. (2012) The ubiquitin code. *Annu. Rev. Biochem.* **81,** 203–229
66. Lim, K.-H., and Baek, K.-H. (2013) Deubiquitinating enzymes as therapeutic targets in cancer. *Curr. Pharm. Des.* **19,** 4039–4052
67. Zhang, Y., Zhou, L., Rouge, L., Phillips, A. H., Lam, C., Liu, P., Sandoval, W., Helgason, E., Murray, J. M., Wertz, I. E., and Corn, J. E. (2013) Conformational stabilization of ubiquitin yields potent and selective inhibitors of USP7. *Nat. Chem. Biol.* **9,** 51–58
68. Bashore, C., Dambacher, C. M., Goodall, E. A., Matyskiela, M. E., Lander, G. C., and Martin, A. (2015) Ubp6 deubiquitinase controls conformational dynamics and substrate degradation of the 26S proteasome. *Nat. Struct. Mol. Biol.* **22,** 712–719
69. Doeppner, T. R., Doehring, M., Bretschneider, E., Zechariah, A., Kaltwasser, B., Müller, B., Koch, J. C., Bähr, M., Hermann, D. M., and Michel, U. (2013) MicroRNA-124 protects against focal cerebral ischemia via mechanisms involving Usp14-dependent REST degradation. *Acta Neuropathol.* **126,** 251–265
70. Peth, A., Kukushkin, N., Bossé, M., and Goldberg, A. L. (2013) Ubiquitinated proteins activate the proteasomal ATPases by binding to Usp14 or Uch37 homologs. *J. Biol. Chem.* **288,** 7781–7790
71. Mirra, S. S., Murrell, J. R., Gearing, M., Spillantini, M. G., Goedert, M., Crowther, R. A., Levey, A. I., Jones, R., Green, J., Shoffner, J. M., Wainer, B. H., Schmidt, M. L., Trojanowski, J. Q., and Ghetti, B. (1999) Tau pathology in a family with dementia and a P301L mutation in tau. *J. Neuropathol. Exp. Neurol.* **58,** 335–345
72. Khatoon, S., Grundke-Iqbal, I., and Iqbal, K. (1992) Brain levels of microtubule-associated protein tau are elevated in Alzheimer's disease: a radioimmuno-slot-blot assay for nanograms of the protein. *J. Neurochem.* **59,** 750–753
73. Götz, J., Xia, D., Leinenga, G., Chew, Y. L., and Nicholas, H. (2013) What renders tau toxic. *Front. Neurol.* **4,** 72
74. Silva, M. C., Cheng, C., Mair, W., Almeida, S., Fong, H., Biswas, M. H., Zhang, Z., Huang, Y., Temple, S., Coppola, G., Geschwind, D. H., Karydas, A., Miller, B. L., Kosik, K. S., Gao, F.-B., *et al.* (2016) Human iPSC-derived neuronal model of tau-A152T frontotemporal dementia reveals tau-mediated mechanisms of neuronal vulnerability. *Stem Cell Reports* **7,** 325–340
75. Pir, G. J., Choudhary, B., Mandelkow, E., and Mandelkow, E.-M. (2016) Tau mutant A152T, a risk factor for FTD/PSP, induces neuronal dysfunction and reduced lifespan independently of aggregation in a *C. elegans* tauopathy model. *Mol. Neurodegener.* **11,** 33
76. Lopez, A., Lee, S. E., Wojta, K., Ramos, E. M., Klein, E., Chen, J., Boxer, A. L., Gorno-Tempini, M. L., Geschwind, D. H., Schlotawa, L., Ogryzko, N. V., Bigio, E. H., Rogalski, E., Weintraub, S., Mesulam, M. M., *et al.* (2017) A152T tau allele causes neurodegeneration that can be ameliorated in a zebrafish model by autophagy induction. *Brain* **140,** 1128–1146
77. Biernat, J., Gustke, N., Drewes, G., Mandelkow, E. M., and Mandelkow, E. (1993) Phosphorylation of Ser262 strongly reduces binding of tau to microtubules: distinction between PHF-like immunoreactivity and microtubule binding. *Neuron* **11,** 153–163
78. Drewes, G., Trinczek, B., Illenberger, S., Biernat, J., Schmitt-Ulms, G., Meyer, H. E., Mandelkow, E. M., and Mandelkow, E. (1995) Microtubule-associated protein/microtubule affinity-regulating kinase ($p110^{mark}$). A novel protein kinase that regulates tau-microtubule interactions and dynamic instability by phosphorylation at the Alzheimer-specific site serine 262. *J. Biol. Chem.* **270,** 7679–7688
79. Damme, M., Suntio, T., Saftig, P., and Eskelinen, E.-L. (2015) Autophagy in neuronal cells: general principles and physiological and pathological functions. *Acta Neuropathol.* **129,** 337–362
80. Son, J. H., Shim, J. H., Kim, K.-H., Ha, J.-Y., and Han, J. Y. (2012) Neuronal autophagy and neurodegenerative diseases. *Exp. Mol. Med.* **44,** 89–98
81. Spilman, P., Podlutskaya, N., Hart, M. J., Debnath, J., Gorostiza, O., Bredesen, D., Richardson, A., Strong, R., and Galvan, V. (2010) Inhibition

of mTOR by rapamycin abolishes cognitive deficits and reduces amyloid-β levels in a mouse model of Alzheimer's disease. *PLoS One* **5,** e9979
82. Weathington, N. M., and Mallampalli, R. K. (2014) Emerging therapies targeting the ubiquitin proteasome system in cancer. *J. Clin. Investig.* **124,** 6–12
83. Wiesner, D. A., and Dawson, G. (1996) Staurosporine induces programmed cell death in embryonic neurons and activation of the ceramide pathway. *J. Neurochem.* **66,** 1418–1425
84. Belmokhtar, C. A., Hillion, J., and Ségal-Bendirdjian, E. (2001) Staurosporine induces apoptosis through both caspase-dependent and caspase-independent mechanisms. *Oncogene* **20,** 3354–3362
85. Rappsilber, J., Ishihama, Y., and Mann, M. (2003) Stop and go extraction tips for matrix-assisted laser desorption/ionization, nanoelectrospray, and LC/MS sample pretreatment in proteomics. *Anal. Chem.* **75,** 663–670
86. MacLean, B., Tomazela, D. M., Shulman, N., Chambers, M., Finney, G. L., Frewen, B., Kern, R., Tabb, D. L., Liebler, D. C., and MacCoss, M. J. (2010) Skyline: an open source document editor for creating and analyzing targeted proteomics experiments. *Bioinformatics* **26,** 966–968
87. Schmittgen, T. D., and Livak, K. J. (2008) Analyzing real-time PCR data by the comparative C_T method. *Nat. Protoc.* **3,** 1101–1108
88. Zhao, W.-N., Cheng, C., Theriault, K. M., Sheridan, S. D., Tsai, L.-H., and Haggarty, S. J. (2012) A high-throughput screen for Wnt/β-catenin signaling pathway modulators in human iPSC-derived neural progenitors. *J. Biomol. Screen.* **17,** 1252–1263
89. Chen, J., Zhou, Y., Mueller-Steiner, S., Chen, L.-F., Kwon, H., Yi, S., Mucke, L., and Gan, L. (2005) SIRT1 protects against microglia-dependent amyloid-β toxicity through inhibiting NF-κB signaling. *J. Biol. Chem.* **280,** 40364–40374